

DISSERTATION

**INVESTIGATING MOLECULAR DETERMINANTS OF FIV PATHOGENESIS**

Submitted by

Jesse Alan Thompson

Department of Microbiology, Immunology, and Pathology

In partial fulfillment of the requirements

for the Degree of Doctor of Philosophy

Colorado State University

Fort Collins, Colorado

Spring 2009

UMI Number: 3374630

### INFORMATION TO USERS

The quality of this reproduction is dependent upon the quality of the copy submitted. Broken or indistinct print, colored or poor quality illustrations and photographs, print bleed-through, substandard margins, and improper alignment can adversely affect reproduction.

In the unlikely event that the author did not send a complete manuscript and there are missing pages, these will be noted. Also, if unauthorized copyright material had to be removed, a note will indicate the deletion.

UMI<sup>®</sup>

---

UMI Microform 3374630  
Copyright 2009 by ProQuest LLC  
All rights reserved. This microform edition is protected against  
unauthorized copying under Title 17, United States Code.

---

ProQuest LLC  
789 East Eisenhower Parkway  
P.O. Box 1346  
Ann Arbor, MI 48106-1346

COLORADO STATE UNIVERSITY

April 7, 2009

WE HEREBY RECOMMEND THAT THE DISSERTATION PREPARED  
UNDER OUR SUPERVISION BY JESSE ALAN THOMPSON ENTITLED  
**INVESTIGATING MOLECULAR DETERMINANTS OF FIV PATHOGENESIS**  
BE ACCEPTED AS FULFILLING IN PART REQUIREMENTS FOR THE DEGREE  
OF DOCTOR OF PHILOSOPHY.

Committee on Graduate Work

  
\_\_\_\_\_

Jonathan O. Carlson

  
\_\_\_\_\_

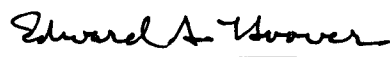
Chaoping Chen

  
\_\_\_\_\_

Sandra L. Quackenbush

  
\_\_\_\_\_

Advisor Susan VandeWoude

  
\_\_\_\_\_

Department Head Edward A. Hoover

ABSTRACT OF DISSERTATION  
INVESTIGATING MOLECULAR DETERMINANTS  
OF FIV PATHOGENESIS

Feline immunodeficiency virus (FIV) is a naturally-occurring lentivirus of domestic cats. Infection results in acquired immunodeficiency syndrome associated with progressive loss of CD4<sup>+</sup> T-lymphocytes. FIV has a similar genome structure as human immunodeficiency virus (HIV), containing several open-reading-frame (ORF) accessory genes, and uses a similar mechanism of cellular entry. Similarities between these complex lentiviruses make FIV infections a relevant animal model for studies of HIV-AIDS.

Five FIV clades have been identified and are distinguished by envelope sequence. Two isolates, FIV-PPR and FIV-CPG (molecular clone FIV-C36), belonging to clades A and C, respectively, are variable with regard to disease potential. Pathology of lentivirus subtypes can be attributed to any number of properties, including replication rates or levels dictated by a combination of viral and host factors; these include viral genome secondary structure, efficacy of evasion of a host innate or adaptive immune response, binding affinity to cell surface receptors, and epigenetic factors. Chimeric viruses constructed between phenotypically distinct strains of FIV are potentially useful tools to identify molecular determinants of virulence. Several chimeric constructs were therefore developed by exchanging elements between FIV-C36 and FIV-PPR.

FIV-PCenv and FIV-PC3'LTR were two resulting chimeras that were capable of competent *in vitro* replication. Studies in Chapter One aimed to characterize these viruses in the domestic cat model and to test the hypothesis that elements surrounding the *env* region contribute to *in vivo* pathology. FIV-PC3'LTR, containing FIV-C36 *rev2* and 3' LTR was infectious, although attenuated compared to parental constructs. FIV-PCenv, containing FIV-C36 *vif*, *orfA*, *env*, and the first exon of *rev*, displayed a phenotype intermediate to parental viruses with regard to replication kinetics, and CD4<sup>+</sup> T-cell and neutrophil declines, but peak viral load and development of clinical disease was delayed by three weeks compared to FIV-PPR, FIV-PC3'LTR, and FIV-C36.

Studies in Chapter Two evaluate potential mechanisms for the delayed phenotype of FIV-PCenv and test whether serial passage of this virus in cats resulted in different viral replication kinetics and pathogenicity *in vivo*. Sequence analysis of provirus recovered from a cat infected with FIV-PCenv at peak proviral load revealed a change in the Rev-response element of FIV-PCenv compared to published FIV-CPG sequences making up chimera inoculum. To test the hypothesis that delayed kinetics observed during FIV-PCenv infections was due to adaptation of the construct during first round infections, pooled plasma from the *in vivo* study described in Chapter One was used to inoculate a second cohort of cats. Control groups were challenged with naïve plasma. Passaged FIV-PCenv again displayed intermediate phenotype in terms of viral replication and immunopathology, but onset of acute viremia was no longer delayed. Both circulating virus and proviral loads were higher than during previous infections with FIV-PCenv, along with more sustained significant decreases in CD4<sup>+</sup> T-cells compared to mock-infected controls. These results support the notion that 3' elements contribute to

heightened virulence observed during FIV-C36 infections, and that passage of FIV-PCenv through cats resulted in virus that was more replication competent than the initial molecularly cloned chimera.

To further pinpoint particular genes that contribute to FIV pathogenesis, three additional chimeras were generated using PCR-driven overlap extension as described in Chapter Three. Overlapping PCR was utilized to produce chimeras with specifically substituted ORF genes encoding the FIV-C36 regulatory proteins Vif and OrfA for those from FIV-PPR; chimeras FIV-PCvif, FIV-PCvif/orfA, and FIV-PCorfA were successfully constructed as determined by sequence analysis of each chimeric virus. Supernatant from Crandell feline kidney cells (CrFK) transfected with plasmids encoding full-length chimeras tested positive for reverse-transcriptase (RT) activity and was used for generation of viral stocks. Upon infection of the feline MYA-1 T-cell line with RT-positive CrFK cell-free supernatant, all three chimeras produced measurable RT activity. Further, *in vitro* analysis of FIV-PCvif/orfA demonstrated that this construct had replication properties equal to those of FIV-C36 as measured by viral capsid and RNA genome production in a cat T-cell line. These constructs will allow for further dissection of viral genomic characteristics that relate to disease phenotype. Ultimately, important information relating to mechanisms of lentiviral pathogenicity may be gleaned from this work, with potential for development of new therapeutic interventions for this and other lentiviral diseases.

Jesse A. Thompson  
Microbiology, Immunology, and Pathology  
Colorado State University  
Fort Collins, CO 80523  
Spring 2009

## TABLE OF CONTENTS

	<u>Page</u>
Signature Page	ii
Abstract	iii
Introduction	1
Feline Immunodeficiency Virus	1
Utility of FIV as a Model for HIV	2
Molecular Biology of FIV	4
Pathology of Various FIV Subtypes	5
Contribution of Regulatory Elements to FIV Lifecycle	7
Chapter 1 – <i>in vivo</i> Infections Using Clade A/C Chimeric FIVs	10
Introduction	10
Materials and Methods	13
Results	16
Discussion	25
Chapter 2 – Further Analysis of Chimeric FIV-PCenv	29
Introduction	29
Materials and Methods	30
Results	35
Discussion	46
Chapter 3 – Generation of FIV Accessory-Gene Chimeras	51
Introduction	51
Materials and Methods	57
Results	62
Discussion	75
Conclusion	78
References	82

## INTRODUCTION

### **Feline Immunodeficiency Virus**

Feline immunodeficiency virus (FIV) is taxonomically classified within family *Retroviridae*, in the genus *Lentivirus*. FIV infects more than a dozen species of *Felidae* (73), as well as domestic cats worldwide. While evidence for clinical disease in wild species remains inconclusive, FIV infection leads to acquired immunodeficiency syndrome (AIDS) in domestic cats (15, 25, 48, 50). Experimentally infected domestic cats develop immune abnormalities (15) which are dose-dependent (21). Initial infection results in high levels of circulating virus, with a corresponding rise in antibody titers, which both decline as infection proceeds. A latent phase occurs which may last weeks to years. Interestingly, the length of the latent period is highly FIV-strain dependent for reasons that have not been clearly elucidated. Feline AIDS is characterized by recrudescence of high levels of circulating virus, progressive loss of CD4<sup>+</sup> T-lymphocytes, neutropenia, weight loss, gingivitis, neurological deficits, and opportunistic infections (3, 15).

Domestic cats are at low risk for FIV exposure if kept indoors; however, risk of contracting the disease increases if they are allowed outside. Feral cats are at highest risk due to increased chance of encountering an FIV-infected individual. Biting and sexual activity are among factors for transmission, as virus is readily isolated from the saliva of infected animals (78), and FIV can be transmitted via the vaginal mucosa (2, 4, 40). Gender and age contribute to incidence; feral males are three times more likely to

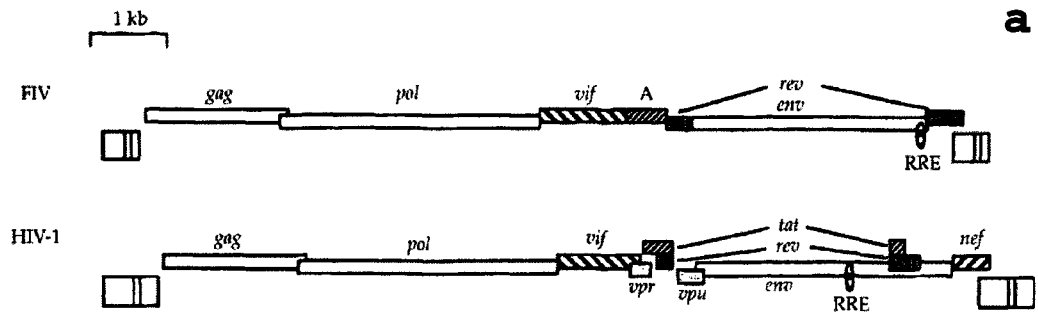
contract FIV than females, and individuals over the age of six have higher rates of infection (77).

Five major FIV subtypes (A-E) have been identified based on phylogenetic analysis of envelope gene (*env*) sequences. Subtypes A and B predominate worldwide and are distributed throughout North America, Europe, Australia, and South Africa (14, 27-29, 65). Subtype C, first isolated in British Columbia (65), has also been reported in Vietnam (42). Phylogenetic evidence gathered thus far geographically restricts the remaining two subtypes, D to Japan (27), and E to Argentina (47). Recent analysis of the V3-V5 region of *env* in virus isolated from cats in Portugal revealed high divergence from any of the previously identified subtypes (14), highlighting the genetic diversity of FIV and likelihood that additional strains are yet to be discovered.

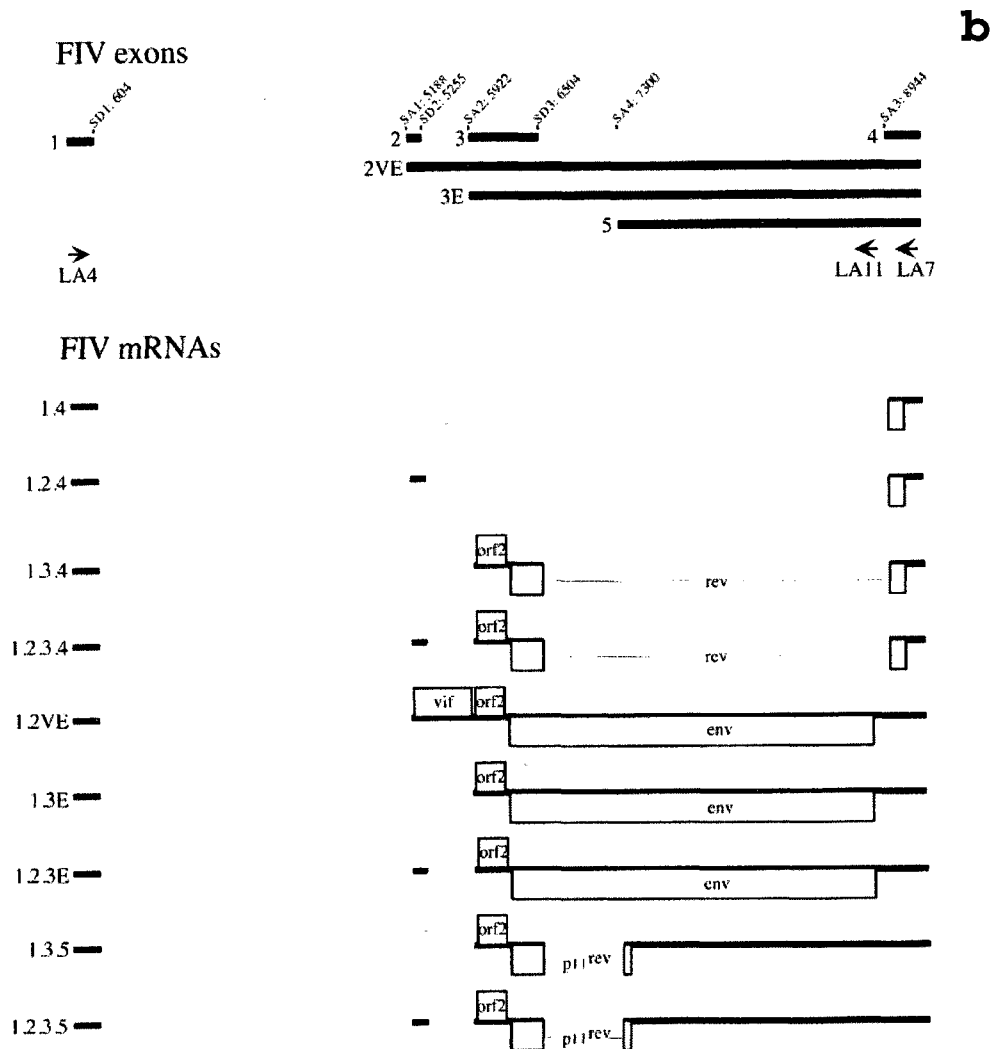
### **Utility of FIV as a Model for HIV**

FIV biology closely resembles that of human immunodeficiency virus-1 (HIV-1) in terms of lifecycle, genomic organization, and pathology (48, 50, 77). Like all retroviruses, HIV and FIV *gag*, *pol*, and *env* are arranged 5'-3' along the genome (**Fig 1**); these encode major structural, enzymatic, and surface precursors, respectively (6). Both FIV and HIV have evolved complex genomes relative to other retroviruses, with regulatory elements that influence host-cell machinery to aid their propagation. These elements are encoded as open-reading-frames (ORFs) within the genome, and in FIV include Vif, OrfA, and Rev.

Transcription of integrated provirus by host RNA polIII is mediated by promoter regions within FIV and HIV long-terminal-repeats (LTRs). Surface and transmembrane



(a) Tomonaga, K., and T. Mikami. 1996. *J Gen Virol* 77:1611-21.



(b) de Parseval, A., and J. H. Elder. 1999. *J Virol* 73:608-17.

**Figure 1:** Genome comparison and open-reading-frame organization of the complex retroviruses FIV and HIV showing major *gag*, *pol*, and *env* genes, along with regulatory, accessory elements (a). Multiple splice patterns of FIV mRNAs, including those encoding *vif*, *orfA*, and *rev* (b).

envelope subunits are post-translationally glycosylated in Golgi vesicles and assemble at the cytoplasmic surface of the plasma membrane. Viral matrix, capsid, and nucleocapsid structural proteins associate with dimeric RNA genomes and are assembled into virus particles which bud from the plasma membrane. Consequently, virion surfaces are composed of host lipids and proteins, in addition to viral envelope subunits.

Vaccination using dual subtype (A and D) inactivated whole virus has been successful in cats experimentally challenged with FIV compared to cats receiving placebo (32), yielding the first commercially- available FIV vaccine, Fel-O-Vax. Effectiveness against a strain belonging to the more ubiquitous subtype B has been demonstrated experimentally (55), further strengthening the potential for Fel-O-Vax to control spread of FIV among the domestic cat population.

Given the structural and replication cycle similarities, and the capacity to induce at least partially-protective immunity against infection using a prophylactic vaccine, FIV-induced immunodeficiency in a natural host offers a unique model for studies in HIV transmission, *in vivo* kinetics, pathology, host immune responses, and host immune dysfunction; in fact, FIV infection of domestic cats represents the only naturally-occurring T-lymphotropic lentiviral disease other than HIV that leads to AIDS.

### **Molecular Biology of FIV**

Full-length FIV transcripts initiated from integrated provirus are destined for either packaging into virions as RNA genomes, or translated as Gag and Pol structural and enzymatic gene products. Capping at the 5' end of mRNAs and 3' polyadenylation are mediated by cellular machinery and occur prior to splicing, thus all FIV transcripts

are capped and polyadenylated (6). At least three singly-spliced mRNA species exist (**Fig 1**), all containing a 5' leader sequence, and are translated as Env subunits or the regulatory proteins Vif and OrfA (10, 69). The remaining multiply-spliced FIV mRNAs discovered to date encode either the Rev protein from two exons, products which display partial Rev activity of nuclear mRNA export (10), or have not been fully characterized. Alternative splicing events bring together distant open-reading frames (ORFs) through association with cellular spliceosome components (6). Small nuclear RNAs (snRNAs), coupled with their corresponding small nuclear ribonucleoproteins (snRNPs), base-pair with pre-mRNAs and direct cleavage in the spliceosome through recognition of splice acceptor and donor consensus sequences within the FIV genome.

### **Pathology of Various FIV Subtypes**

Like HIV, subtype classifications referred to as clades have been established for FIV (65). Clades are most typically distinguished by nucleotide sequence of hypervariable regions, and are therefore based on *env*, which mutates to the greatest degree due to the battle between viral evolution and host immune recognition and pressure (65).

Similar to primate lentiviruses, FIV exhibits structural and functional diversity that dictates *ex vivo* and *in vivo* growth rates, host-cell range, and *in vivo* pathogenesis. The majority of FIV subtypes identified fall into clades A or B and exhibit varying degrees of pathogenicity in animals (65). In contrast, at least one clade C isolate causes a much higher disease incidence and severity, with approximately 60% mortality within 18 weeks post-infection (13, 45). Further, when directly compared to the clade A isolate

FIV-Petaluma, the clade C isolate FIV-PGammar replicates to higher titers during experimental infections (49). Circulating FIV, along with proviral load, are markedly elevated during these infections (49). Additionally, hallmarks of immunodeficiency, including lymphopenia, neutropenia, and opportunistic infections, occur earlier and to a greater degree (49). Infections with the molecular clone of FIV-PGammar (FIV-C36) result in severe acute immunodeficiency disease in young cats (11). Interestingly, a dam nursing FIV-C36 infected kittens became infected following natural exposure and developed high viral load, demonstrating for the first time lentivirus transfer from offspring to parent (11).

Surface glycoproteins of a lentivirus dictate specificity for host-cell receptors as well as binding affinity. Differential abilities to recognize, bind, and fuse with the primary receptor CD134 (9, 63) and the co-receptor CXCR4 (57, 75) may define the variable host-cell range and pathogenesis observed during infections with distinct FIV strains. Envelope surface units are the target for host surveillance, and are therefore under constant pressure to evade an antibody response. Additionally, regulatory proteins expressed from overlapping reading frames adjacent to and within *env* are targets for innate intracellular antiviral responses. Thus, the battle between virus and host can lead to selection of mutations, resulting in emergence of a quasispecies possessing attributes advantageous to viral propagation that are able to avoid host immune defenses. Variants capable of unchecked replication typically cause more virulent infections. Provided the important roles for surface glycoproteins and regulatory elements, it is logical to evaluate the *env* region when exploring molecular determinants of FIV pathogenesis.

## **Contribution of Regulatory Elements to FIV Lifecycle**

Productive FIV infections depend on the proper expression and function of regulatory proteins. Genes encoding viral infectivity factor (Vif), open-reading-frame A (OrfA), and the Rev protein are positioned along the 3' half of the viral genome. FIV and HIV each express Vif and Rev, while there is evidence that FIV OrfA and HIV Tat (5, 10) or Vpr (16, 17) serve similar functions. These regulatory, accessory proteins are translated from multiply spliced mRNAs (10, 72). Properties attributed to FIV envelope and accessory genes can be further explored as a means to discover HIV treatment modalities.

**FIV-Vif.** Vif is essential for FIV replication (35, 71) and affects the ability of FIV to establish infections in naïve cells. It has been shown convincingly that human apolipoprotein B-editing catalytic polypeptide 3 (APOBEC3) proteins, normally packaged into virions, are instead bound by HIV Vif and targeted for proteosomal degradation (7, 37, 61, 79). The requirement for FIV Vif is likely linked to sequestration of feline APOBEC3s (feAPOBECs), cellular factors from the cytidine deaminase family of proteins. Three feAPOBEC3s have been identified in CrFK cells: APOBEC3C, APOBEC3H, and APOBEC3CH (41). Inhibition of feAPOBEC deaminase activity by the feline foamy virus (FFV) Bet protein has been demonstrated (34). FIV Vif expression also results in reduced mutation rates (46), leading to the hypothesis that like HIV Vif and FFV Bet, FIV Vif directly binds feAPOBECs, preventing their incorporation into mature virions and effectively stopping extensive G-to-A mutations from occurring in the integrated provirus of a newly infected cell (41, 46, 54).

**FIV-OrfA.** Evidence suggests that FIV OrfA may function as a transcriptional transactivator similar to HIV Tat (5, 10), though it has also been shown to function similar to HIV Vpr as an enhancer of viral infectivity and virion formation (16, 17). Transcription rates or levels may be enhanced via direct binding of the *orfA* gene product to secondary structure within the viral LTR promoter, similar to HIV Tat interactions with the TAR region (6). Although a specific mechanism for viral enhancement has not been elucidated, it is known that HIV Vpr localizes to the plasma membrane, and although it is not a structural protein, is packaged into virions (6). Arguably, either of these scenarios would be reasonable given that FIV *orfA* and both HIV *tat* and *vpr* are located in the same region of their respective genomes. Recently, microarray data has been used to show that OrfA expression affects cellular factors associated with post-transcriptional modification and protein ubiquitination pathways (68).

**FIV-Rev and the RRE.** The regulatory protein Rev, through interactions with the Rev response element (RRE), facilitates export of unspliced and singly-spliced viral transcripts across the nuclear membrane (6). The RRE is around 150 nucleotides in length, forming a secondary structure in the 3' end of *env* and extending into the non-coding region (51). Upon disruption of the RRE, Rev function is inhibited (38).

Unspliced cellular pre-mRNAs are bound by small nuclear ribonucleoprotein particles (snRNPs) and are prevented from leaving the nucleus. These snRNP complexes also inhibit movement of full-length viral transcripts across the nuclear pore. Simpler retroviruses contain a constitutive transporter element (CTE) sequence that binds cellular mRNA transporters with high affinity. Complex retroviruses such as HIV and FIV have

evolved the Rev:RRE mechanism to overcome this barrier to nuclear export of viral mRNAs.

Current molecular biology techniques allow for construction of genetic chimeras. Given the relatively small genome of FIV ( $\approx 9$  Kb), it is not a daunting task to implement restriction endonuclease or PCR-mediated techniques to exchange portions of one viral genome with another. Using this technology, questions aimed at determining which genomic elements are responsible for lentiviral pathogenicity can be evaluated. Characterization of FIV chimeras in the domestic cat model can map molecular determinants of virulence, thereby opening avenues toward a deeper understanding of immunodeficiency-inducing lentiviruses, along with discovery of therapies that target FIV and HIV.

## CHAPTER ONE

### *in vivo* Infections Using Clade A/C Chimeric FIVs

#### INTRODUCTION

Understanding the molecular determinants that play a role in lentiviral replication and pathogenesis is highly significant for development of intervention strategies relevant to treatment of AIDS in both cat and human. As with primate lentiviruses, the molecular basis for the varied pathogenic potential of different FIV isolates is not fully understood, despite the fact that in addition to variable host responses, viral genomic structure is highly related to disease outcome. This has been well demonstrated in the FIV model system wherein there occurs significant variation in disease outcome following infections with different FIV molecular clones, including FIV-PPR and FIV-C36 (11, 12, 52, 66).

Molecular clones of the relatively neuropathogenic, clade A isolate FIV-PPR (52) and the highly immunopathogenic, clade C clone FIV-C36 (11) were used to test whether viral LTR transcription efficiencies were responsible for the heightened pathogenesis observed during clade C FIV infections. No significant differences were noted in activity levels of chloramphenicol acetyl-transferase (CAT) when driven by the two viral LTRs (12), suggesting that LTR transcription initiation does not account for functional disparity. Furthermore, binding assessment of FIV-PPR and FIV-C36 Env to the primary cell surface receptor CD134 (9, 63), or the chemokine co-receptor CXCR4 (57, 75), failed to distinguish the two clones (12). These experiments suggest that cellular entry and rate of transcription were not primary mechanisms underlying the variations in pathogenicity between parental molecular clones.

A pilot study was conducted for twelve weeks to confirm *in vivo* infectivity of chimeric FIV-PCenv and FIV-PC3'LTR (n=2/group). Data was accumulated by Dr. Wendy Sprague. Immunoblot analysis demonstrated seroconversion in all cats by six weeks PI (data not shown). Further, both PBMC provirus and circulating FIV were detected in both groups of animals infected with chimeric FIVs (data not shown).

We undertook the present study as an approach to elucidate which genetic elements contribute to the pathogenic phenotype of FIV-C36. A panel of clade A/C chimeric FIVs between FIV-PPR and FIV-C36 were generated and used to infect the T cell line 104-C1, unsorted feline peripheral blood mononuclear cells (PBMCs), or primary CD4<sup>+</sup> and CD8<sup>+</sup> T-lymphocytes (12). Based on *ex vivo* infectivity, we chose two chimeric constructs (**Fig 1.1**) for further analysis *in vivo*. We report here a comparison of infection parameters of chimeras FIV-PCenv and FIV-PC3'LTR relative to each other and to the parental strains FIV-PPR and FIV-C36 during the early course of infection in domestic cats.

Genetically, FIV-PPR and FIV-C36 share 80% nucleotide identity within the 3' region encompassing *env*, from start of *vif* to end of *rev2*. Provided this 20% variation, it is logical to hypothesize that recognition of variable Env epitopes by host antibodies provides FIV-C36 with the ability to evade an antiviral response more effectively than FIV-PPR, leading to its heightened virulence. In the same respect, amino acid coding sequence may dictate higher performance and efficiency of FIV-C36 regulatory proteins over those of FIV-PPR. These considerations further strengthen the need to evaluate *env* for factors that influence *in vivo* viral replication and related pathology.

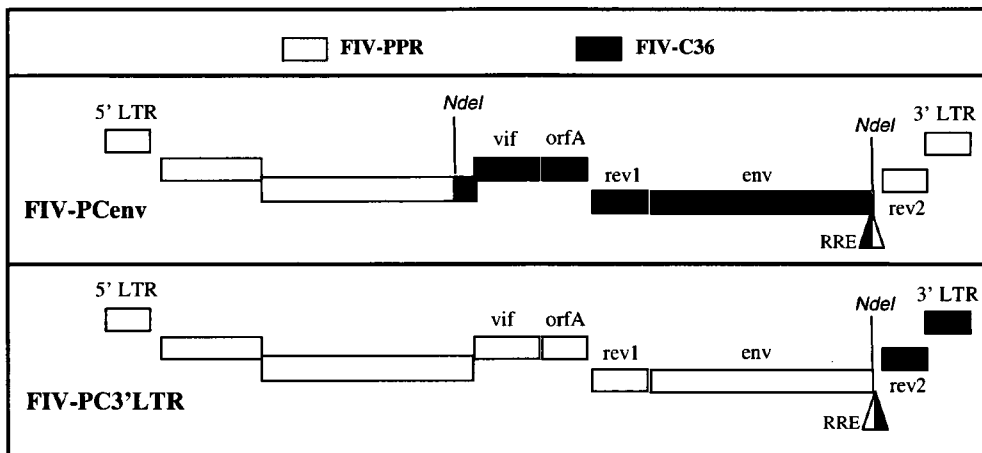


**Figure 1.1:** Clade A/C FIV chimeras. Clade C FIV-C36 sequences are depicted in black, and clade A FIV-PPR sequences in white. Recombinant clone FIV-PCenv was generated by exchanging ~5kb of FIV-C36 between the *Nde*I restriction endonuclease recognition sites. FIV-PC3'LTR contains FIV-C36 3'LTR including the second exon of *rev*.

## MATERIALS AND METHODS

**Generation of constructs.** Constructs for these initial studies were generated and tested by Dr. Sohela de Rozières in the laboratory of Dr. John Elder at The Scripps Research Institute (TSRI) as described (12). Briefly, full-length parental plasmid clones (FIV-PPR and FIV-C36) were used to generate chimeras. Both parental clones possess a common *NdeI* restriction site at nucleotide (nt) 8899. A second *NdeI* restriction site (silent mutation at nt 5000) was introduced into wild type FIV-PPR by site-directed mutagenesis. This allowed a swapping of the *NdeI* fragments containing the FIV *vif*, *orfA* and *env* genes, along with the first exon of *rev*, to produce FIV-PCenv (**Fig 1.1**). Similarly, the shared *NdeI* site was used to substitute the second exon of *rev*, along with the 3' LTR, to produce FIV-PC3'LTR (**Fig 1.1**). Chimeric clones were transformed in MAX Efficiency® Stbl2™ competent *E. coli* (Invitrogen, Carlsbad, CA) in order to avoid LTR-mediated instability and recombination of lentiviral sequences. Constructs were verified for correct sequences by restriction enzyme analysis, and direct sequencing by TSRI Center for Nucleic Acid Research. Receptor binding studies and *ex vivo* replication analysis summarized above were also performed at TSRI.

***in vivo* infections.** Twenty-four 14-16 week-old, specific pathogen free (SPF) cats were housed in gang rooms in AAALAC-international accredited Colorado State University (CSU) animal facilities following protocols approved by CSU Animal Care and Use Committee (ACUC). Ten animals were born in the CSU SPF breeding colony, and fourteen were obtained from a commercial SPF colony (Cedar River Laboratories, Ames, IA). We inoculated four groups of unanesthetized, age and sex-matched cats

(n=5) of either FIV-PPR, FIV-PCenv, FIV-PC3'LTR, or FIV-C36 generated after one round of replication in feline PBMC. Four cats were administered media only as non-infected controls. Animals were monitored daily for clinical signs of illness. We measured weights, and collected blood on days -7, 7, 10, 14, 21, 30, 35, 42, 62, 77, 102, 132, and 156 post-inoculation (PI) for detection of circulating virus and PBMC provirus, along with hematologic analysis. Bone marrow aspirates were performed on ketamine/acepromazine anesthetized animals on days 42, 77, and 156 PI for detection of provirus.

**Hematologic analysis.** To determine percentage of cells positive for CD4 and CD8 surface antigens, we added 30  $\mu$ l of EDTA anti-coagulated blood to 12 x 75 mm polystyrene tubes, along with 0.15  $\mu$ l of FITC-labeled mouse monoclonal anti-CD4 and 0.3  $\mu$ l of PE-labeled mouse monoclonal anti-CD8 (Southern Biotech, Birmingham, AL) diluted in FACS buffer (5% BSA, 0.1% sodium azide in PBS). Next, samples were incubated for 30 min at room temperature. Red blood cells were lysed by Q-prep (Beckman Coulter, Miami, FL), and flow cytometry performed on a CyAn cell sorter (Dako Cytomation, Glostrup, Denmark). We analyzed results using Summit software package (Dako Cytomation). To determine complete leukocyte and RBC counts from EDTA blood, we used a Z1 Series Coulter Counter. Differential leukocyte counts were determined manually from stained smears. Absolute neutrophil and lymphocyte counts were calculated by multiplying the total leukocyte count by the percentages of neutrophils or lymphocytes for each cat at each time point. To determine absolute CD4<sup>+</sup> and CD8<sup>+</sup> cell counts, total lymphocyte counts were multiplied by percentage of FITC

(CD4) or PE (CD8) fluorescing cells. We collected blood from all cats 7 days prior to infection to establish baseline values.

**Statistics.** To analyze decreases in CD4 and neutrophil counts, and CD4:CD8 ratios for infection groups compared to controls at each time point, GraphPad Prism® (La Jolla, CA) was used to determine one-tailed P values in an unpaired t test. P values below 0.05 were considered significant.

**FIV proviral DNA and plasma RNA quantitation.** Plasma was collected from EDTA-treated whole blood following centrifugation and frozen at -70°C until processing. RNA was purified from 140 µl of plasma using a QIAamp Viral RNA Mini Kit (Qiagen, Valencia, CA). SuperscriptII (Invitrogen) was implemented in reactions with random hexamers (Invitrogen) added, and treated with RNase Out (Invitrogen) for preparation of cDNA from viral RNA. Genomic DNA was extracted from PBMCs purified on a Histopaque-1077 (Sigma, St. Louis, MO) gradient. Cells were washed and pellets frozen at -20°C overnight. DNA was isolated using a DNeasy Tissue Kit (Qiagen).

Real-time PCR was performed on an iCycler thermocycler (Bio-Rad, Hercules, CA) to detect both proviral and circulating FIV *gag* using the AmpliTaq Gold DNA polymerase-containing TaqMan Universal PCR Master Mix (Applied Biosystems, Foster City, CA). Sequences of primer/ probe (5'FAM, 3'TAMRA) sets are reported in (49) and were as follows: FIV-A, f=GCCTTCTCTGCAAATTTAACACCT, r=GATCATATTCTGTGTCAGTTGCTTT, and p=TGCGGCCATTATTAATGTGGC CATG. FIV-C, f=ACTCACCCCTCCTGATGGTCCTA, r=TGAGTCAGCCCTATCCCC

ATTA, and p=ACCATTGCCATACTTCACTGCAGCCG. PCR reactions in a total volume of 25  $\mu$ l consisted of 12.5  $\mu$ l master mix, 0.5  $\mu$ l each of 20  $\mu$ M forward and reverse primers, 0.2  $\mu$ l of 10  $\mu$ M probe, and 5  $\mu$ l template. After 2 min at 50°C, the AmpliTaq Gold DNA polymerase was activated at 95°C for 10 min, followed by 45 cycles of 95°C for 15s and 60°C for 1 min.

Threshold cycle values (CT) were defined as the point at which the fluorescence passed a threshold limit. FIV proviral copy number was calculated using a standard curve generated from dilutions of a sub-cloned *gag* PCR product. To calculate copy number of viral RNA in plasma, we used a standard curve that was generated by diluting FIV-PPR virus stock in naïve cat plasma and prepared and analyzed by reverse-transcriptase quantitative PCR as described above. CT values were compared to those of the sub-cloned *gag* standard to assign values. Lower limits of detection approached 10 RNA or DNA equivalents. Characteristics of samples in this range included CT values over 40, higher standard deviation between replicates, or detectable signal in only one or two of three replicates.

## RESULTS

Results from the pilot study demonstrated the ability of FIV-PCenv and FIV-PC3'LTR to establish productive infections *in vivo*. Based on these findings, a large-scale comparative study lasting twenty-two weeks was conducted using more animals per group (n=5) in which parental FIV-PPR and FIV-C36 were tested alongside FIV-PCenv and FIV-PC3'LTR.

**in vivo kinetics of FIV-PCenv and FIV-PC3'LTR.** Relative levels of viremia were assessed over time by measuring both the number of viral RNA copies per milliliter plasma and the number of viral DNA copies detected per  $10^6$  PBMC DNA equivalents. During infections with parental viruses and FIV-PC3'LTR, average numbers of viral RNA copies per milliliter peaked at day10 PI (FIV-PPR), or day14 PI (FIV-C36 and FIV-PC3'LTR), whereas FIV-PCenv demonstrated delayed kinetics, with viral load not peaking until day 35 PI (**Fig 1.2**).

FIV-C36 infections resulted in greatest peak viremia with levels reaching  $6.17 \times 10^7$  copies/ml. Peak circulating viral load was nearly as high for FIV-PCenv as for FIV-PPR with levels reaching  $2.76 \times 10^4$  and  $7.37 \times 10^4$  copies/ml, respectively. FIV-PC3'LTR was attenuated compared to both parental constructs, reaching  $9.37 \times 10^3$  copies/ml. At time of necropsy, FIV-PC3'LTR plasma loads were lowest, averaging 52 copies/ml, followed by FIV-PPR which averaged  $1.17 \times 10^3$  copies/ml. FIV-PCenv and FIV-C36 retained higher levels of  $8.21 \times 10^3$  and  $2.86 \times 10^4$  RNA copies/ml, respectively, by study end on day 156 PI (**Fig 1.2**). All animals displayed plasma viremia during study course; however, two FIV-PC3'LTR infections resulted in transient viremia between days 14-21 PI and on day 132 PI, while remaining time points for these cats were negative, attributing to lower group means.

Integrated proviral *gag* sequences were detected in PBMC by day 7 PI in all cats inoculated with parental constructs, between days 7 and 14 PI in FIV-PC3'LTR infections, and between days 10-42 in FIV-PCenv infections. Proviral load peaked by day 35 PI in all cats infected with FIV-C36, FIV-PPR, and FIV-PC3'LTR. FIV-PCenv

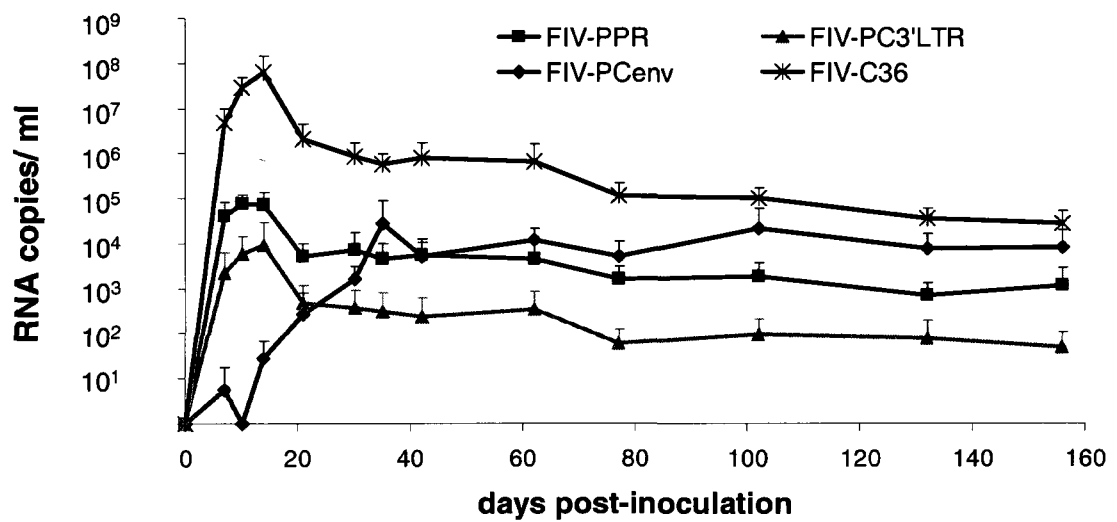


**Figure 1.2:** Circulating virus during infections with wild-type clades A and C and A/C chimeric FIVs. Group averages for plasma viremia are shown as numbers of RNA genomes/ml over the course of the 156 day study. PCR reactions were performed in triplicate. Mock-infected cats had undetectable viremia (data not shown).

did not attain maximal proviral load until day 77 PI , and were comparable to those of FIV-PPR at that time (**Fig 1.3a**). Mean peak numbers of proviral copies/ $10^6$  PBMCs remained relatively constant for all groups until study end and were as follows: FIV-PC3'LTR=  $5.88 \times 10^2$ , FIV-PPR=  $3.47 \times 10^3$ , FIV-PCenv=  $6.53 \times 10^3$ , and FIV-C36=  $1.35 \times 10^5$  (**Fig 1.3a**).

*Detection of provirus in bone marrow.* Bone marrow was collected on days 42, 77, and 156 PI. Using quantitative real-time PCR, we detected proviral *gag* DNA in all infection groups at all time points. Number of bone marrow-positive cats within each group for each collection day are reported in **Table 1.1**. As in peripheral blood, initial FIV-C36 values were the highest, followed by FIV-PPR, then FIV-PC3'LTR, and lastly FIV-PCenv (**Fig 1.3b**). Similar to observations in peripheral blood FIV-PCenv showed delayed kinetics, with DNA copies per million cells equaling FIV-PPR values by day 156 PI.

At the time of the first sampling (day 42 PI), mean bone marrow loads for all strains with the exception of FIV-PCenv which was lower, were equivalent to those observed in peripheral blood. Mean FIV-PPR bone marrow loads were relatively equal to those of PBMC at all time points. However, average FIV-C36 and FIV-PC3'LTR bone marrow provirus levels declined over time relative to PBMC. Interestingly, number of FIV-PCenv integrations in bone marrow increased over time (**Table 1.1**).

*Hematologic effects of FIV-PCenv and FIV-PC3'LTR infections.* Absolute CD4<sup>+</sup> T lymphocyte counts pre-infection were normal ( $>1000/\mu\text{L}$ ) and similar to controls

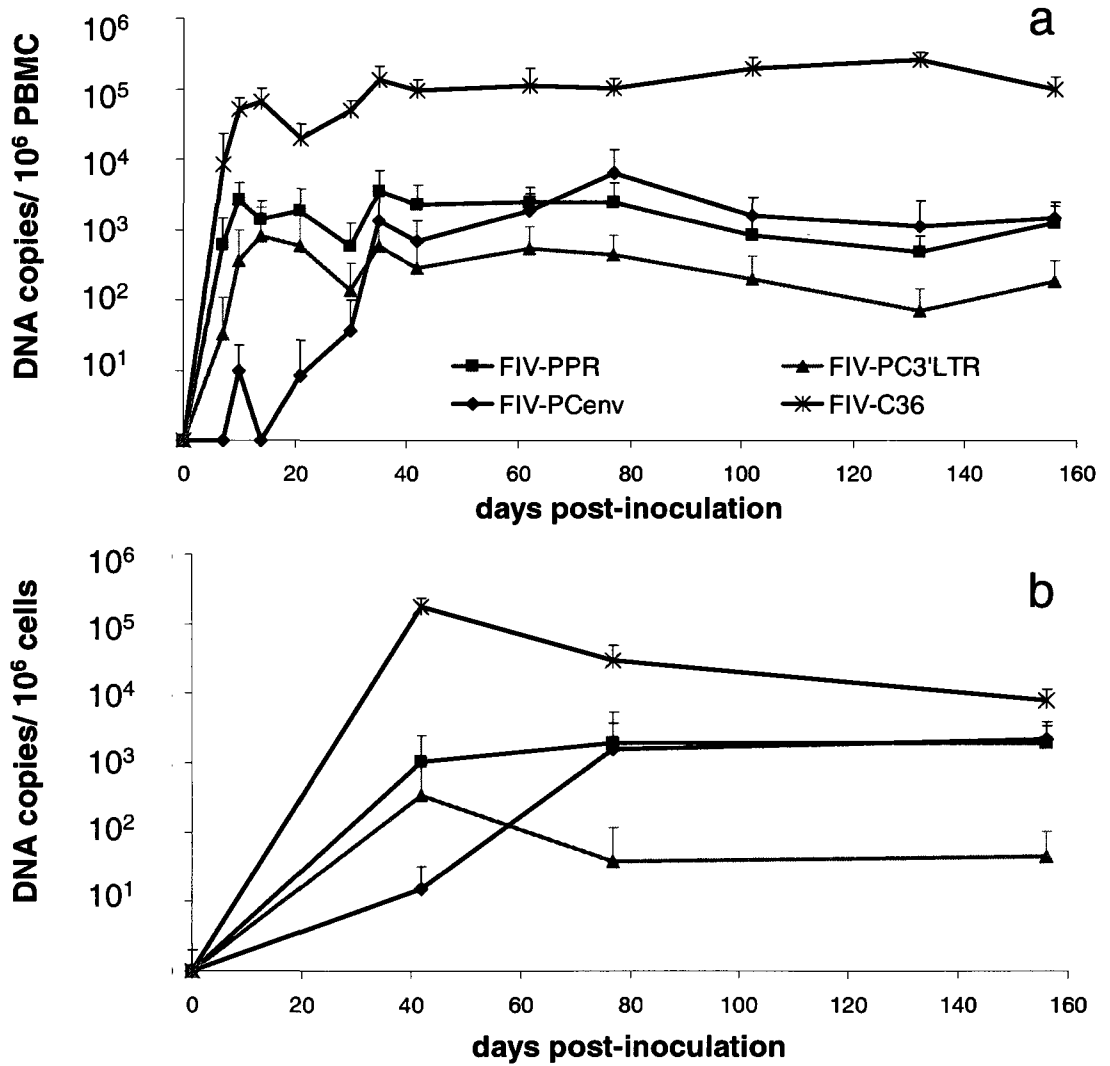


**Figure 1.3:** PBMC (a) and bone marrow (b) proviral loads during infections with parental and chimeric FIVs. Group averages are shown as numbers of FIV *gag* equivalents/10<sup>6</sup> cells over the course of the 156 day study. PCR reactions were performed in triplicate. Mock-infected cats were provirus-negative (data not shown).

	day 42 PI		day 77 PI		day 156 PI	
	PBMC	BM	PBMC	BM	PBMC	BM
FIV-PPR	2.26E+03	1.05E+03	2.43E+03	1.90E+03	1.26E+03	1.91E+03
FIV-PC3'LTR	2.86E+02	3.47E+02	4.47E+02	3.88E+01	1.85E+02	4.41E+01
FIV-PCenv	6.95E+02	1.51E+01	6.53E+03	1.56E+03	1.48E+03	2.20E+03
FIV-C36	9.34E+04	1.74E+05	1.02E+05	3.01E+04	9.98E+04	8.07E+03
		# cats BM+		# cats BM+		# cats BM+
		4/5		5/5		5/5
		3/5		3/5		4/5
		3/5		3/5		5/5
		5/5		5/5		5/5

**Table 1.1:** Actual mean levels of PBMC and bone marrow proviral loads in cats infected with FIV-PPR, PC3'LTR, PCenv, or C36 (as shown in fig 1.3). Bone marrow samples were taken on days 42, 77, and 156 PI. FIV gag was detected and recorded as numbers of proviral equivalents/10<sup>6</sup> cells. Number of bone marrow-positive cats is shown for each time point. All cats were PBMC-positive during these time points.

in all groups (**Fig 1.4a**). FIV-C36 infected cats tended to have early and significant declines in CD4<sup>+</sup> T cells that stabilized by day 77 PI. CD4<sup>+</sup> T cell counts in FIV-PCenv-infected cats were significantly lower than those in controls at day 62 ( $P = 0.037$ ), and in two of five cats, levels dropped below 1,000/ $\mu$ L by day 102 PI, maintaining this depletion until study end, at which time group mean CD4<sup>+</sup> T-cell level was significantly lower than for controls ( $P = 0.002$ ) (**Fig 1.4a** and **1.5a**). In comparison, CD4<sup>+</sup> T cell depletions observed in FIV-PPR and FIVPC3'LTR-infected cats were delayed and milder. CD4:CD8 ratio declines reflected CD4<sup>+</sup> T cell depletion, i.e. FIV-C36 infected cats had the lowest ratios through the study starting at day 30 PI, and after day 60, FIVPCenv CD4:CD8 were below control levels. FIV-PPR and FIVPC3'LTR levels remained above or consistent with control means for the entire study (**Fig 1.4b** and **1.5b**). Toward study end, the ratio for FIV-C36 infections dropped more sharply than in other cats due to an increase in absolute CD8<sup>+</sup> T cell numbers (data not shown).

Neutropenia in cats is typically defined by circulating neutrophil values lower than 2000/ $\mu$ L. While neutrophil decline was observed in some FIV-PPR (4/5) and FIV-PC3'LTR (3/5) infected cats, and in two of five non-infected cats, it was mild and transient, with numbers remaining above 1000/ $\mu$ L (**Fig 1.4c**). All five FIV-C36 infected cats experienced marked neutropenia starting at day 30 PI which was statistically significant ( $P < 0.0001$ ) compared to non-infected controls (**Fig 1.4c** and **1.5c**). Three of these animals recovered by study end, while two remained neutropenic throughout the study. FIV-PCenv infections also resulted in prolonged neutropenia in three cats, appearing between days 77 and 102 PI and persisting until study end (**Fig 1.4c** and **1.5c**).

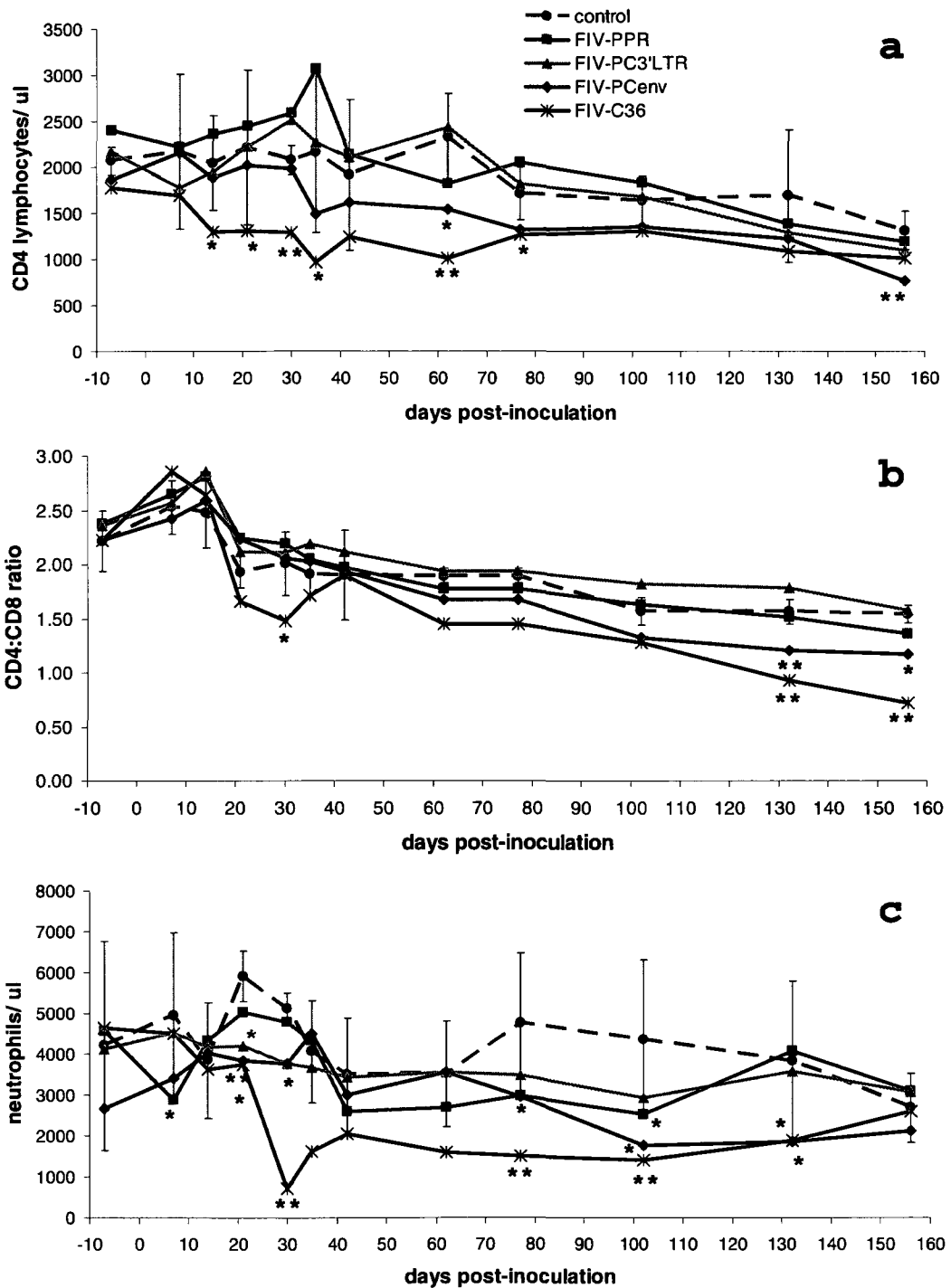


**Figure 1.4:** Timecourse of hematologic changes in domestic cats infected with parental or chimeric FIVs. Blood was sampled at various time points over the course of infection. Complete blood counts, differential leukocyte analysis, and CD4<sup>+</sup> and CD8<sup>+</sup> T-lymphocyte percentages in virus-inoculated cats (n=5/group), or sham-inoculated control cats (n=4) were calculated. CD4 counts (shown as number of cells/ $\mu$ l) (a), CD4:CD8 ratios (b), and neutrophil counts (shown as cells/ $\mu$ l) (c) are demonstrated over the course of the study. For ease of viewing, error bars are shown for control group only. Statistically significant values relative to normal control values are indicated by asterisks (\*,  $P$  between 0.01 and 0.05; \*\*,  $P < 0.01$ ).

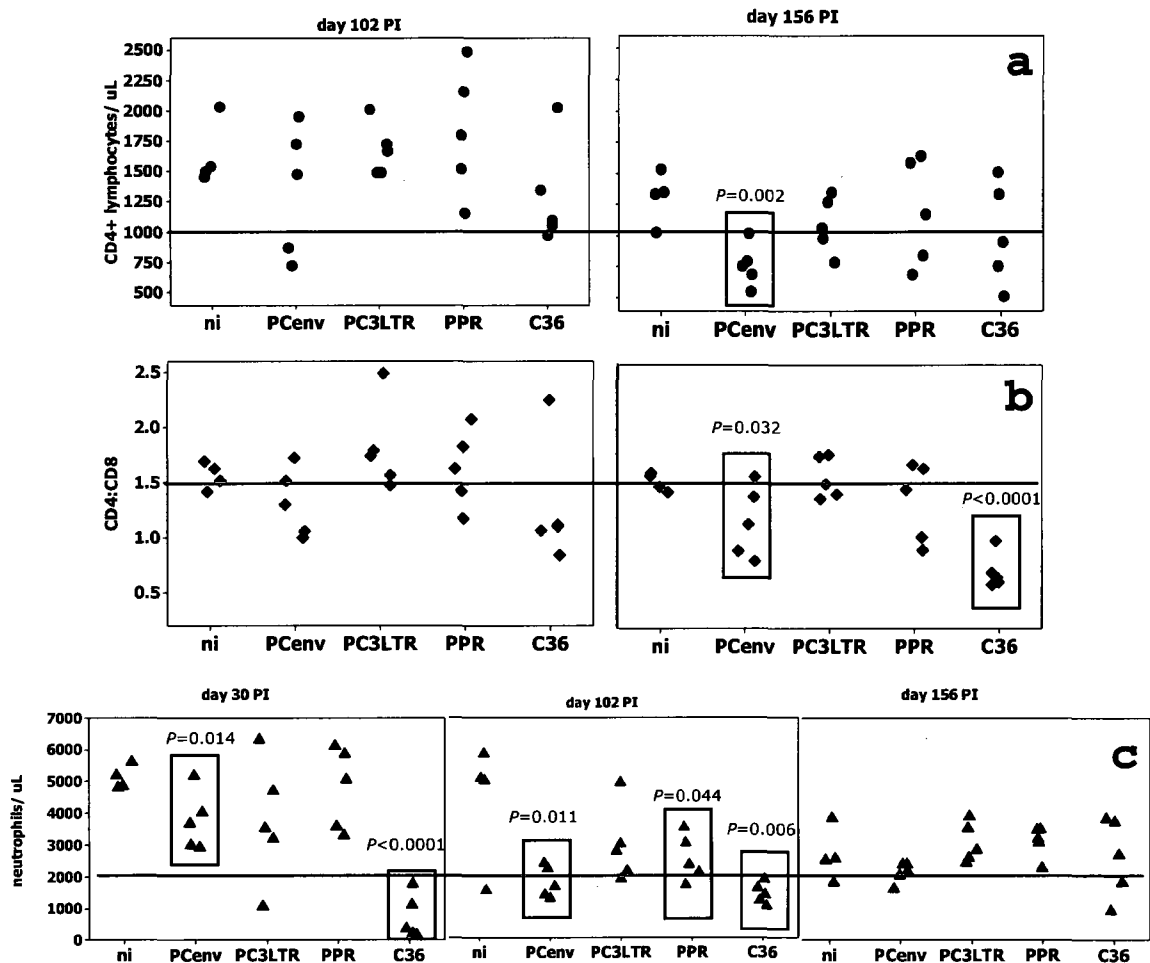


**Figure 1.5:** Peripheral T-cell and neutrophil kinetics for individual cats infected with parental or chimeric FIVs. Blood was sampled at various time points over the course of infection. While group means were not always statistically different (Fig 1.4), individual animal measurements illustrated at days 102 and 156 PI demonstrate trends for CD4 depletion (a) and CD4:CD8 ratio decrease (b) in FIV-C36 and FIV-PCenv vs levels in other groups. Further, neutrophil counts at days 30, 102, 156 PI demonstrate neutropenia in FIV-C36 and FIV-PCenv vs levels in other groups (c). For ease of viewing, reference points are illustrated by horizontal bars placed at 1000 CD4+ T-cells/ $\mu$ l, a CD4:CD8 ratio of 1.5, and 2000 neutrophils/ $\mu$ l. ni, no infection (control).

As noted in figure 1.4c, group means were statistically lower than controls on days 21, 30, 77 (FIV-C36 only), 102, and 132 PI during FIV-C36 and FIV-PCenv infections.

## DISCUSSION

We generated chimeras between two strains of FIV (FIV-PPR and FIV-C36) in an attempt to determine contributions of molecular determinants to the distinct pathologies of these isolates. FIV-PCenv is a construct in which the 3' portion of FIV-C36 had been swapped with that of FIV-PPR, while FIV-PC3'LTR contained the second exon of *rev* and the 3' LTR of FIV-C36 on the FIV-PPR background. To define the unique replication properties of two distinct strains of FIV, we performed *in vivo* infections to compare infectivity and pathogenicity of the two chimeric constructs relative to those of parental strains. Even with clade C components, neither FIV-PCenv nor FIV-PC3'LTR chimeras exhibited the accelerated disease phenotype of FIV-C36. FIV-PC3'LTR was attenuated, while FIV-PCenv had characteristics intermediate to those of the parental viruses.

Results from experiments performed *ex vivo* indicated that the difference in observed replication rates between FIV-PPR and FIV-C36 could not be explained simply due to differential promoter/enhancer strength (12). In addition, no significant differences were observed in the ability of the two viruses to utilize CD134 and CXCR4 as receptors (12). Further, substitutions in which FIV-C36 elements were included on the FIV-PPR genome did not substantially increase replicative capacity *ex vivo*, even when FIV-C36 *env* was substituted for that of FIV-PPR (12). Replicative capacity of FIV-PCenv and FIV-PC3'LTR during infections of PBMC and sorted CD4<sup>+</sup> and CD8<sup>+</sup> T-

lymphocytes prompted their *in vivo* characterization. Factors lacking in an *ex vivo* setting but present in the feline model could influence functional domains of the FIV genome included on these chimeras. For instance, 5' and 3' LTR promoter elements present in FIV-PC3'LTR mediate transcription that may be aided by the *orfA* gene product. Surface and transmembrane envelope units are crucial to receptor binding, and would be tested as a fully functional modality in a live animal using FIV-PCenv.

Our study showed that viral kinetics and virulence characteristics of FIV-C36 and FIV-PPR molecular clones *in vivo* were similar to those observed previously for both cloned and uncloned field isolates (11, 49, 66). FIV-C36 displayed an accelerated disease phenotype when compared to FIV-PPR during infections of domestic cats. Plasma viremia, along with PBMC proviral load, peaked at the same time PI for parental viruses, but reached much higher levels in FIV-C36 infections. Additionally, depletion of peripheral CD4<sup>+</sup> T lymphocytes and neutrophils was early and dramatic during FIV-C36 infections, while FIV-PPR infected cats tended to have relatively stable counts compared to uninfected controls.

While the FIV-PC3'LTR chimera was less robust *in vivo* than either parental construct, suggesting this substitution resulted in decreased fitness, FIV-PCenv dynamics were unique in exhibiting delayed replication and plateau phase kinetics, along with hematologic effects that were intermediate between parental strains. This observation may indicate that this chimera gained an enhanced replicative capacity during the course of infection and suggests that the FIV-C36 genomic elements *vif*, *orfA*, and *env*, and a portion of the *rev* response element may contribute to *in vivo* virulence phenotype. Lagging viral loads may indicate initial immune pressure on a virus which contains FIV-

C36 elements that need to adapt to FIV-PPR counterparts. FIV-PCenv, due to its engineered nature, is presumably less efficient at overcoming defenses mounted by the host, leading to a longer incubation period for a diverse number of quasispecies to arise.

The ability of FIV-C36 to replicate to high titer and induce neutropenia may be dictated by cell susceptibility mediated through envelope subunits or accessory proteins encoded in the *env* region. Comparing sequence of FIV-PCenv isolated from infected cats relative to inoculum sequence will aid to support these conclusions by tracking nucleotide changes and comparing them to parental sequences. It will also be of interest to determine whether *in vivo* passage of FIV-PCenv increases its pathogenicity, similar to observations using HIV/simian immunodeficiency virus (SHIV) chimeras (56), and to evaluate viral genome correlates with such a phenomenon.

Given the observations that LTR promoter activity and receptor binding between FIV-PPR and FIV-C36 were similar, it seems plausible that FIV-C36 may be less prone to host restrictive factors known to inhibit retroviral replication. For example, the Trim 5 $\alpha$  class of proteins that block uncoating of capsid and inhibit cDNA transcription of viral sequences in primate lentiviruses (19, 58, 67). Human and rhesus macaque monkey Trim 5 $\alpha$  proteins have been shown to restrict FIV infection (58), implying that similar mechanisms occur during FIV infection. Higher net replication rates may be attributed to successful bypassing or surviving Trim 5 $\alpha$  restriction, allowing intact FIV-C36 to reach the cell nucleus with greater ease and speed, thus leading to better integration, transcription, and assembly of virions.

Although inclusion of FIV-C36 Vif did not impart clade C growth potential to the chimeric FIVs studied here, a more efficient interaction with the family of feAPOBEC

molecules may also contribute to increased subtype C replication by reducing cytidine deamination in newly synthesized viral DNA (41). Additional innate levels of control during viral infection that may also be factors that influence relative FIV replication rates will likely be discovered.

Subsequent studies presented in Chapters Two and Three will explore these possibilities by testing the replicative capacity and ability to cause decreases in CD4<sup>+</sup> T-cells and neutrophils during *in vivo* passage of FIV-PCenv. Production of chimeras containing FIV-C36 accessory genes on the FIV-PPR backbone will also be described. These can be tested as a means to further pinpoint viral genetic factors responsible for FIV pathogenesis.

## CHAPTER TWO

### Further Analysis of Chimeric FIV-PCenv

#### INTRODUCTION

As described in Chapter One, the pathogenic phenotype of FIV-PCenv was delayed during *in vivo* infections, but it ultimately bore similarities to parental virus FIV-C36 (12). This suggests that FIV-C36 genomic elements within the chimera are in some way related to pathogenicity. It is possible that the delayed viral replication kinetics, and the lag time in CD4<sup>+</sup> T-cell and neutrophil decreases, resulted from FIV-PCenv adaptation within the host or selection of a mutant chimera that was more competent at replication. FIV-C36 portions of the genome must work in conjunction with those of FIV-PPR, and it is likely that a number of replication events are needed in order for FIV-PCenv to gain the heightened fitness that is reflected by increases in circulating viral load and immunocyte dyscrasias. Increases in pathogenicity of HIV/SIV (SHIV) chimeras have been reported during *ex vivo* (33, 36) and *in vivo* passages in macaques (56). Further, quasispecies diversity with respect to receptor usage and host-cell range are broadened upon viral passage (31), supporting this hypothesis.

In this report, we extend our previous studies of the molecular determinants of FIV virulence. We examined the question of whether delayed pathogenicity of FIV-PCenv was an inherent phenotype of its manipulated genome, or if elements near the *env* region contribute to enhanced virulence after a period of adaptation. To test the hypothesis that FIV-PCenv has adapted during primary infections, we performed sequence analysis of proviral DNA from an FIV-PCenv infected cat during a time point

of peak viremia. A nucleotide change within the RRE from the parental chimera was noted in a series of proviral isolates amplified by PCR and sequenced. Evaluation of the secondary structure induced by this mutation predicted a reversion from that of FIV-C36 to FIV-PPR. Whether this reversion is influenced by host or viral factors is unknown; however, RRE interactions with the chimeric Rev protein of FIV-PCenv may be enhanced given this change, explaining the delay in virulence.

To test our hypothesis that an inherent property of the chimeric virus resulted in the unusual delayed kinetics of viral replication, a second cohort of domestic cats were inoculated with pooled plasma from the first group of FIV-PCenv infections to evaluate the impact of serial passage of virus. Upon *in vivo* passage of FIV-PCenv, virus replication as indicated by plasma viremia was not delayed compared to parental strains. Viremia ultimately plateaued in the same range observed in cats infected with FIV-C36, surpassing FIV-PPR levels. Actual numbers of circulating FIV-PCenv RNA genomes, along with PBMC and bone marrow provirus, were elevated during serial passage when compared to primary infection. This effect was not observed during serial passage of parental constructs, again suggesting that some adaptation occurred between passages of FIV-PCenv.

## **MATERIALS AND METHODS**

**Cloning and analysis of FIV-PCenv sequences.** FIV-PCenv stock was used as described in Chapter One to infect cat# 8155 both orally and intravenously with  $10^{3.5}$  TCID<sub>50</sub> particles/ml total (0.5 ml each route). Genomic DNA was extracted from day 77 PI PBMCs purified on a Histopaque-1077 (Sigma) gradient. Cells were washed and

pellets frozen at -20°C overnight. DNA was isolated using a DNeasy Tissue Kit (Qiagen). Using DNA from time of peak viremia (day 77 PI) as template, we amplified three products from the 3' portion of FIV-PCenv, encompassing the entire FIV-C36 portion of the chimera (**Fig 2.1**). PCR conditions were 30 cycles of denaturation at 94°C for 1 min., annealing at 57°C for 30 sec., and extension at 71°C for 1 min. Primer sequences were as follows: f1=GGGTAGAATAGGGGGAATGG, r1=GCCTTACCTTGTCCTGCATA, f2=CCAGAAGAGGCAGAGGAATT, r2=CTGTTCTGCTCCTGCAATG, f3=CAACAGATTGGGGTTACATG, and r3=TGAGTCATGTTTCAGCTGTTTCC. Products were separated on an agarose gel containing ethidium bromide, excised, and purified using the QIAquick gel extraction and purification kit (Qiagen). We used a TOPO TA cloning kit with pPCR2.1 vector (Invitrogen), transforming Top10 *E. coli*, to propagate FIV-PCenv sequences. Colonies were screened via restriction enzyme and PCR analyses, and Qiagen mini-prep kits used to purify plasmid DNA for sequencing at TSRI Center for Nucleic Acid Research. To obtain sequence alignments of six clones for each primer set, we used Sequencher™ software (Gene Codes Corporation, Ann Arbor, MI). Online computer software was used to generate predicted RNA secondary structures (RNAfold, University of Vienna Institute for Theoretical Chemistry), and to translate nucleotide to amino acid sequences (ExPASy, Canadian Bioinformatics Resource).

***in vivo* infections.** Twenty 14-16 week-old, SPF cats were housed in gang rooms in AAALAC-international accredited CSU animal facilities following protocols approved by CSU ACUC. We inoculated three groups (n=5) of unanesthetized cats intravenously

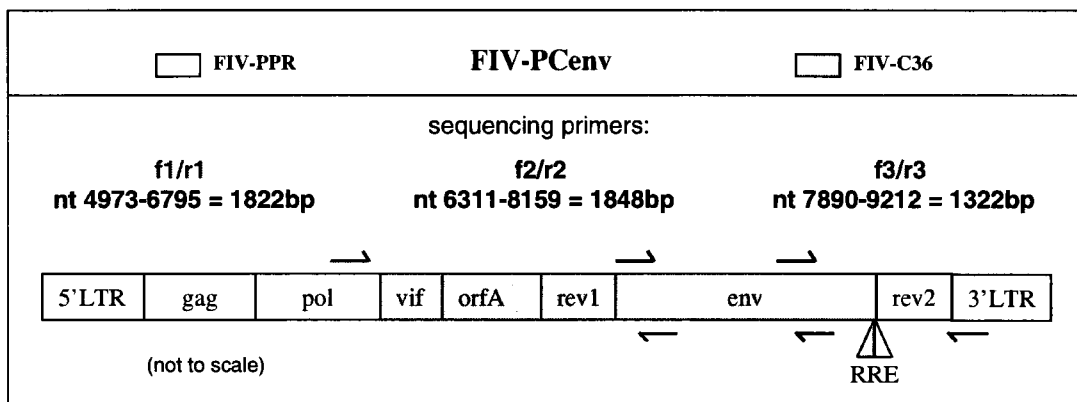


**Figure 2.1:** Schematic showing primer touchdown sites and expected lengths of products amplified for sequence analysis of the FIV-PCenv chimera from cat# 8155 day 77 PI. FIV-PPR regions are depicted in white; FIV-C36, encompassing *vif*, *orfA*, *rev1*, partial RRE, and *env*, in gray.

with 1 ml pooled plasma of five cats previously infected with either FIV-PPR, FIV-PCenv, or FIV-C36. Plasma from time point of peak viremia for each virus (based on RT-PCR values) was used, and normalized using pre-inoculation naïve plasma from matched animals so that all animals received an equal number of viral particles ( $1.38 \times 10^4$ ). Five cats were administered naïve plasma and used as non-infected controls. Animals were monitored daily for clinical signs of illness. We measured weights, and collected blood on days -7, 3, 7, 10, 14, 17, 21, 28, 35, 46, 55, 67, 81, 95, 111, 138, 173, 216, and 259 PI for detection of circulating virus and PBMC provirus, along with hematologic analysis. Two cats from FIV-PPR and FIV-C36 groups were euthanized early prior to day 173 PI due to severe allergies; one received steroid therapy for the symptoms. Bone marrow aspirates were performed on ketamine/acepromazine anesthetized animals on days 3, 17, 35, 55, 95, 173, and 260 PI for detection of provirus.

**Hematologic analysis.** To determine percentage of cells positive for CD4 and CD8 surface antigens, we added 30  $\mu$ l of EDTA anti-coagulated blood to 12 x 75 mm polystyrene tubes, along with 0.15  $\mu$ l of FITC-labeled mouse monoclonal anti-CD4 and 0.3  $\mu$ l of PE-labeled mouse monoclonal anti-CD8 (Southern Biotech) diluted in FACS buffer. Next, samples were incubated for 30 min at room temperature. Red blood cells were lysed by Q-prep (Beckman Coulter), and flow cytometry performed on a CyAn cell sorter (Dako Cytomation). We analyzed results using Summit software package (Dako Cytomation). To determine complete leukocyte and RBC counts from EDTA blood, we used a Z1 Series Coulter Counter. Differential leukocyte counts were determined manually from stained smears. Absolute neutrophil and lymphocyte counts were

calculated by multiplying the total leukocyte count by the percentages of neutrophils or lymphocytes for each cat at each time point. To determine absolute CD4<sup>+</sup> and CD8<sup>+</sup> cell counts, total lymphocyte counts were multiplied by percentage of FITC (CD4) or PE (CD8) fluorescing cells. We collected blood from all cats prior to infection to establish baseline values.

**Statistics.** To analyze decreases in CD4 and neutrophil counts, and CD4:CD8 ratios for infection groups compared to controls at each time point, GraphPad Prism® (La Jolla, CA) was used to determine one-tailed P values in an unpaired t test. P values below 0.05 were considered significant.

**FIV proviral DNA and plasma RNA quantitation.** Plasma was collected from EDTA-treated whole blood following centrifugation and frozen at -70°C until processing. RNA was purified from 140 µl of plasma using a QIAamp Viral RNA Mini Kit (Qiagen). SuperscriptII (Invitrogen) was implemented in reactions with random hexamers (Invitrogen) added, and treated with RNase Out (Invitrogen) for preparation of cDNA from viral RNA. Genomic DNA was extracted from PBMCs purified on a Histopaque-1077 (Sigma, St. Louis, MO) gradient. Cells were washed and pellets frozen at -20°C overnight. DNA was isolated using a DNeasy Tissue Kit (Qiagen).

We performed real-time PCR on an iCycler thermocycler (Bio-Rad) to detect both proviral and circulating FIV *gag* using the AmpliTaq Gold DNA polymerase-containing TaqMan Universal PCR Master Mix (Applied Biosystems). Sequences of primer/ probe (5'FAM, 3'TAMRA) sets are reported in (49) and were as follows: FIV-A, f=GCCTTC

TCTGCAAATTTAACACCT, r=GATCATATTCTGTCAGTTGCTTT, and p=TGCGGCCATTATTAATGTGGCCATG. FIV-C, f=ACTCACCCCTCCTGATGGTCCTA, r=TGAGTCAGCCCTATCCCCATTA, and p=ACCATTGCCATACTTCACTGCAGCCG. PCR reactions in a total volume of 25 µl consisted of 12.5 µl master mix, 0.5 µl each of 20 µM forward and reverse primers, 0.2 µl of 10 µM probe, and 5 µl template. After 2 min at 50°C, the AmpliTaq Gold DNA polymerase was activated at 95°C for 10 min, followed by 45 cycles of 95°C for 15s and 60°C for 1 min.

Threshold cycle values (CT) were defined as the point at which the fluorescence passed a threshold limit. We calculated copy number for FIV provirus using a standard curve generated from dilutions of a sub-cloned *gag* PCR product. To calculate copy number of viral RNA in plasma, we used a standard curve that was generated by diluting FIV-PPR virus stock in naïve cat plasma and prepared and analyzed by reverse-transcriptase quantitative PCR as described above. CT values were compared to those of the sub-cloned *gag* standard to assign values. Identical standard curves to those from the initial study were used, so values obtained for this study were directly comparable to those reported in Chapter One. Lower limits of detection approached 10 RNA or DNA equivalents. Characteristics of samples in this range included CT values over 40, higher standard deviation between replicates, or detectable signal in only one or two of three replicates.

## RESULTS

***FIV-PCenv sequence analysis.*** For amplification and analysis of provirus from an FIV-PCenv infected cat, we chose the time point at which group mean levels were

highest (day 77 PI). This sample was chosen because the likelihood of detecting nucleotide differences compared to inoculum would be greatest after the initial lag period displayed by the chimera. Cat# 8155, the animal with highest number of FIV equivalents per million PBMC ( $1.68 \times 10^4$ ), was chosen. Primers were designed to amplify the FIV-C36 region of FIV-PCenv (**Fig 2.1**). Consensus sequence of six clones per region amplified was aligned with that of virus stock used as inoculum (as determined by electronic database). Sporadic differences were noted for all three regions in some clones; however, only one point mutation was identified in all clones analyzed. Figure 2.2 demonstrates a single nucleotide mutation from adenine to guanine in region three. This change results in loss of a loop in the predicted secondary structure of the RRE from circulating virus in cat# 8155 compared to inoculum. This A→G change also results in reformation of a larger loop seen in parental FIV-PPR, but not FIV-C36 or FIV-PCenv used as inoculum (**Fig 2.3**).

***in vivo passage of FIV-PCenv.*** To test if the delayed viral loads resulting from first round infections of domestic cats were indicative of an initial period of virus adaptation that could be overcome with serial passage, pooled plasma from infected cats was used as inoculum for second round *in vivo* infections. Five cats per group were injected intravenously with plasma containing either FIV-PCenv, FIV-C36, or FIV-PPR, or naïve plasma. Relative rates and levels of viremia were assessed over time by measuring both the number of viral RNA copies per milliliter plasma and the number of viral DNA copies detected per  $10^6$  PBMC DNA equivalents. Initial spikes of viral RNA copies/ml occurred 17-21 days PI for all infection groups (**Fig 2.4**) and were highest in

## FIV-PCenv RRE secondary structures

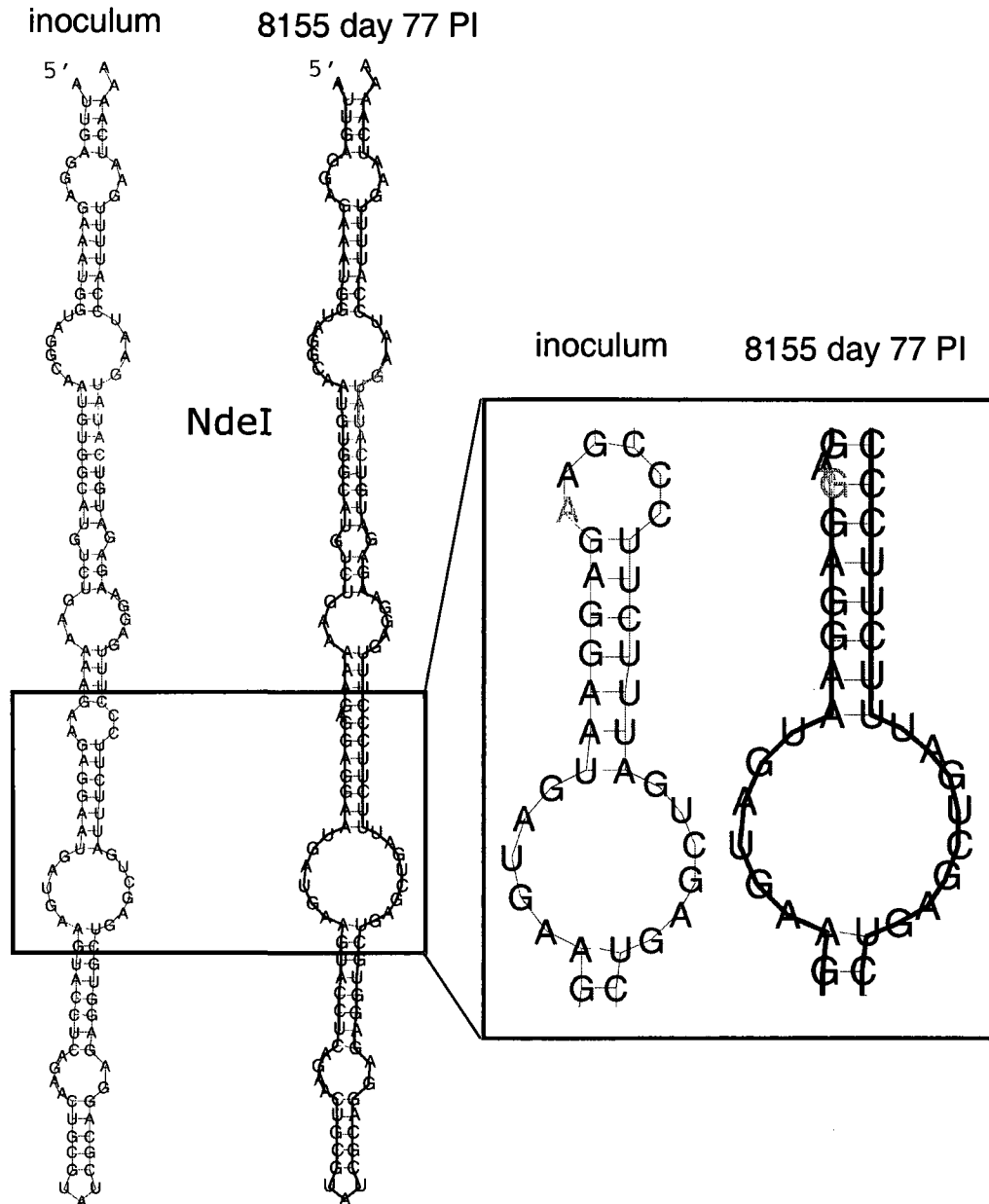


**Figure 2.2:** Predicted secondary structure of the Rev-response element (RRE) of FIV-PCenv mRNA using RNAfold online software. Nucleotide sequence analysis revealed an adenine to guanine mutation in virus isolated from an FIV-PCenv infected cat (8155) on day 77 PI compared to previously published inoculum sequence. NdeI restriction site is highlighted in yellow and denotes chimeric junction. A total of six clones were analyzed to generate a consensus sequence.

## FIV RRE secondary structures

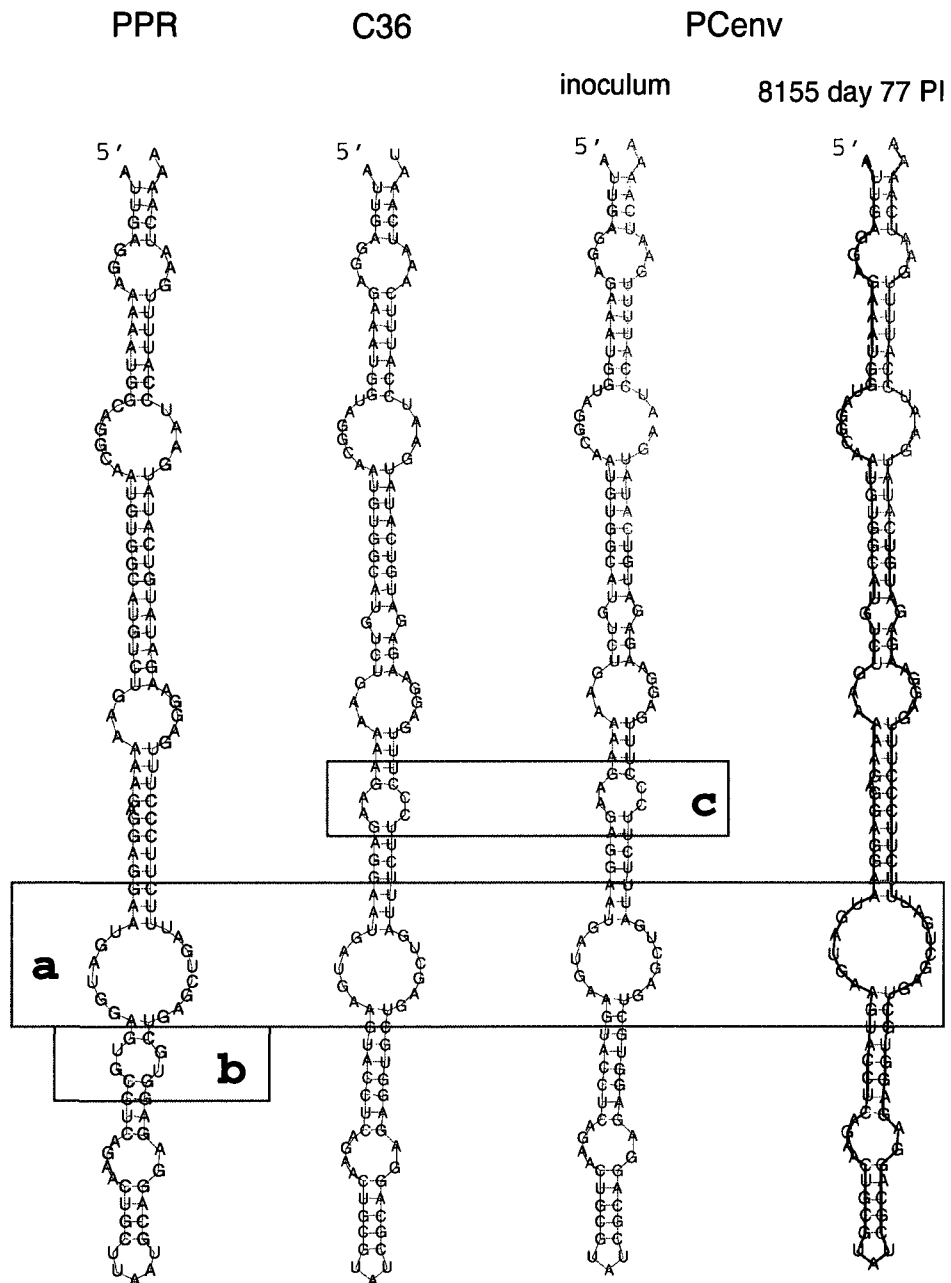


**Figure 2.3:** An adenine to guanine mutation in virus isolated from an FIV-PCenv infected cat (8155) at day 77 PI predicts reversion to a larger loop contained within FIV-PPR (a). This change does not, however, result in gain of smaller loops seen in the molecular clones FIV-PPR (b), or FIV-C36 (c). Highlighted bases in FIV-PCenv denote FIV-PPR origin.

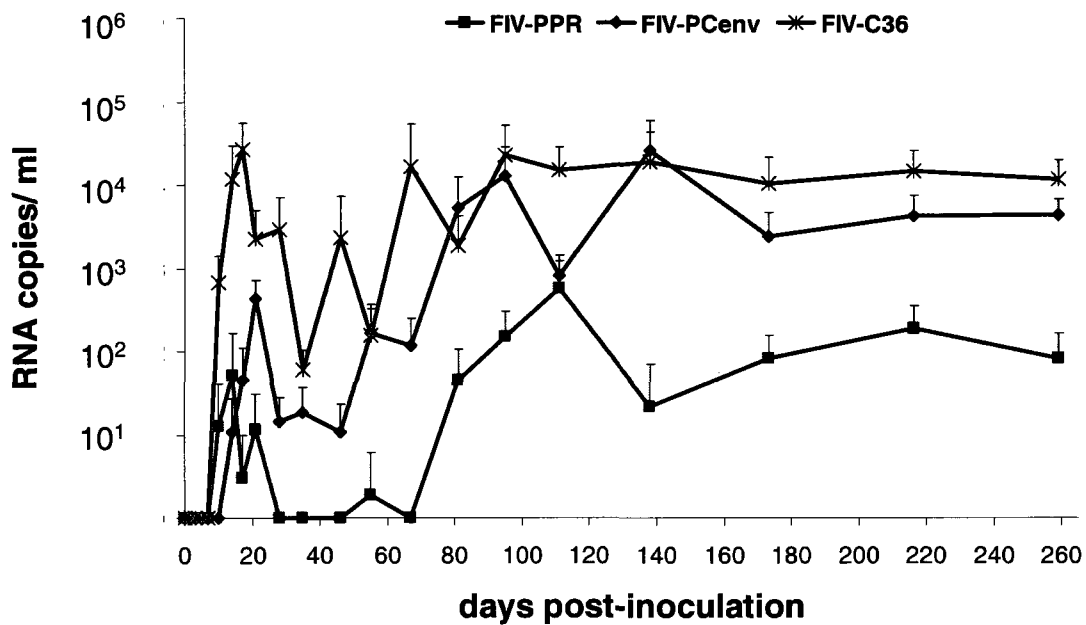


**Figure 2.4:** Circulating virus during *in vivo* passage of clade A FIV-PPR, clade C FIV-C36, and A/C chimeric FIV-PCenv. Group averages for plasma viremia are shown as numbers of RNA copies/ml over the course of the study. PCR reactions were performed in triplicate. Mock-infected cats had undetectable viremia (data not shown).

FIV-C36, followed by FIV-PCenv, then FIV-PPR. Circulating virus levels fluctuated for a period after this initial spike for all groups, with most FIV-PPR values below the level of detection until day 81 PI. In fact, two of five FIV-PPR infected cats were aviremic for nearly six months, until day 173 PI. Maximum mean levels of plasma viremia were detected between three and five months PI for all groups, remaining relatively constant until day 259 PI and were as follows (RNA copies/ ml plasma): FIV-PPR=  $5.68 \times 10^2$ , FIV-PCenv=  $2.58 \times 10^4$ , and FIV-C36=  $2.26 \times 10^4$  (**Fig 2.4**).

FIV-PCenv proviral kinetics in PBMC or bone marrow were similar to circulating virus following *in vivo* passage. Every cat tested positive for integrated proviral *gag* sequence that was detectable in PBMCs on day 14, with an initial spike on day 17 for all constructs; FIV-C36 levels were highest, while FIV-PPR and FIV-PCenv levels were equivalent (**Fig 2.5a**). Mean proviral copies/  $10^6$  PBMCs were highest at 3 to 4 months PI. These values remained relatively constant for all groups as follows: FIV-PPR=  $2.4 \times 10^4$ , FIV-PCenv=  $1.14 \times 10^5$ , and FIV-C36=  $3.55 \times 10^5$  (**Fig 2.5a**).

These trends were reflected in bone marrow, with FIV-PCenv levels remaining intermediate until time of the last biopsies, when they were equal to those of FIV-C36 (**Fig 2.5b**). Two FIV-PPR cats had undetectable bone marrow proviral FIV on day 17 PI; of these, one remained negative until between days 35 and 55 PI. One FIV-PCenv cat had undetectable bone marrow FIV at day 35 PI sampling (**Table 2.1**). Otherwise, all bone marrow samples tested were positive. Compared to PBMC levels, DNA copies/  $10^6$  bone marrow cells were higher on day 173 and 260 PI (**Fig 2.5** and **Table 2.1**), perhaps indicative of a potential reservoir for a latent phase in which virus resides in a site away from the periphery in the midst of less mature activators of immunity.

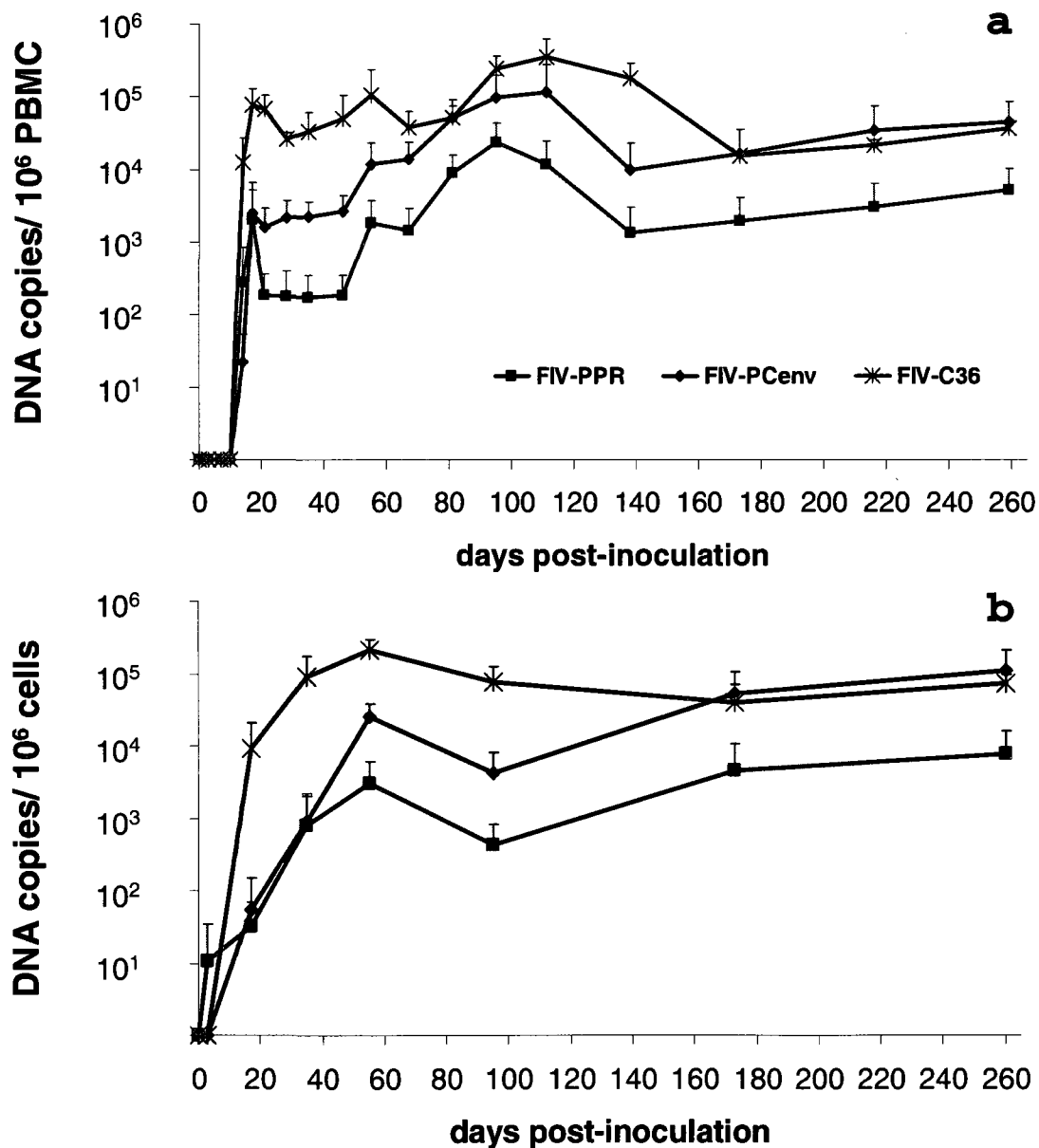


**Figure 2.5:** PBMC (a) and bone marrow (b) proviral loads during *in vivo* passage of FIV-PPR, FIV-C36, and FIV-PCenv. Group averages are shown as numbers of FIV gag equivalents/10<sup>6</sup> cells over the course of the study. PCR reactions were performed in triplicate. Mock-infected cats were provirus-negative (data not shown).

	PBMC	day 17 PI BM	# cats BM+	PBMC	day 35 PI BM	# cats BM+	PBMC	day 55 PI BM	# cats BM+
FIV-PPR	2.02E+03	3.21E+01	3/5	1.72E+02	8.01E+02	4/5	1.81E+03	3.05E+03	5/5
FIV-PCenv	2.52E+03	5.48E+01	5/5	2.27E+03	9.03E+02	4/5	1.19E+04	2.56E+04	5/5
FIV-C36	7.85E+04	9.27E+03	5/5	3.36E+04	9.13E+04	5/5	1.03E+05	2.09E+05	5/5

	PBMC	day 95 PI BM	# cats BM+	PBMC	day 173 PI BM	# cats BM+	PBMC	day 260 PI BM	# cats BM+
FIV-PPR	2.40E+04	4.30E+02	5/5	1.96E+03	4.52E+03	4/4	5.27E+03	7.95E+03	4/4
FIV-PCenv	9.94E+04	4.25E+03	5/5	1.61E+04	5.28E+04	4/4	4.44E+04	1.12E+05	4/4
FIV-C36	2.43E+05	7.78E+04	5/5	1.51E+04	4.00E+04	4/4	3.63E+04	7.29E+04	3/3

**Table 2.1:** Actual mean levels of PBMC and bone marrow proviral loads in cats infected with FIV-PPR, PCenv, or C36 (as shown in fig 2.5). Bone marrow samples were taken on days 3, 17, 35, 55, 95, 173, and 260 PI. FIV gag was detected and recorded as numbers of proviral equivalents/10<sup>6</sup> cells. On day 3 PI, only one FIV-PPR cat had signal in bone marrow which was at the lower level of detection for the assay (10 copies). Number of bone marrow-positive cats is shown for each time point. All cats were PBMC-negative on day 3 PI, two FIV-PPR cats were PBMC-negative on day 17, remaining time points were PBMC-negative for all cats in all groups. One cat each from FIV-C36 and FIV-PPR groups were euthanized early due to severe allergies, while 4/5 samples were obtained from FIV-PCenv group on days 173 and 260 PI, and 3/4 from FIV-C36 group on day 260 PI, explaining lower number tested.

Viral loads were delayed during primary infection with FIV-PCenv; however, upon *in vivo* passage, this delay was not observed compared to wild-type clones. Onset of acute viremia during primary infection versus viral passage are highlighted in figure 2.6. After initial spike, passaged FIV-PCenv provirus continued to rise, reaching maximum levels of DNA copies/  $10^6$  PBMC that were one order of magnitude higher ( $10^5$  versus  $10^4$ ) than levels exhibited during primary infection described in Chapter One (**Fig 2.6a**). Similarly, maximum passaged FIV-PPR levels were on the order of  $10^4$ , compared to  $10^3$  recorded during primary infections, but unlike FIV-PCenv, diminished over time (**Fig 2.6b**). This trend was not observed for FIV-C36 (**Fig 2.6c**). Additionally, maximum levels of circulating virus during FIV-PCenv passage were equal to values observed during primary infection, but lower during passage of parental FIVs. These changes in relative rates and levels of viremia may indicate the emergence of a population of more fit viral progeny.

**Hematologic effects of passaged FIV-PCenv.** During viral passage, onset of CD4<sup>+</sup> T-lymphocyte decreases was similar to primary infections with FIV-C36 and FIV-PCenv; statistically significant differences between infected cats and non-infected controls were observed starting on days 17 and 63 PI, respectively, and persisting through day 138 PI (**Fig 2.7a**). FIV-PPR passage also resulted in significant CD4<sup>+</sup> T-cell drops starting at day 95 PI and persisting through day 138 PI. These declines were reflected in CD4:CD8 ratios (**Fig 2.7b**).

Mean neutrophil counts for all infection groups remained within normal ranges, never dropping below 2000 cells/ $\mu$ l (clinical feline neutropenia), with no significant

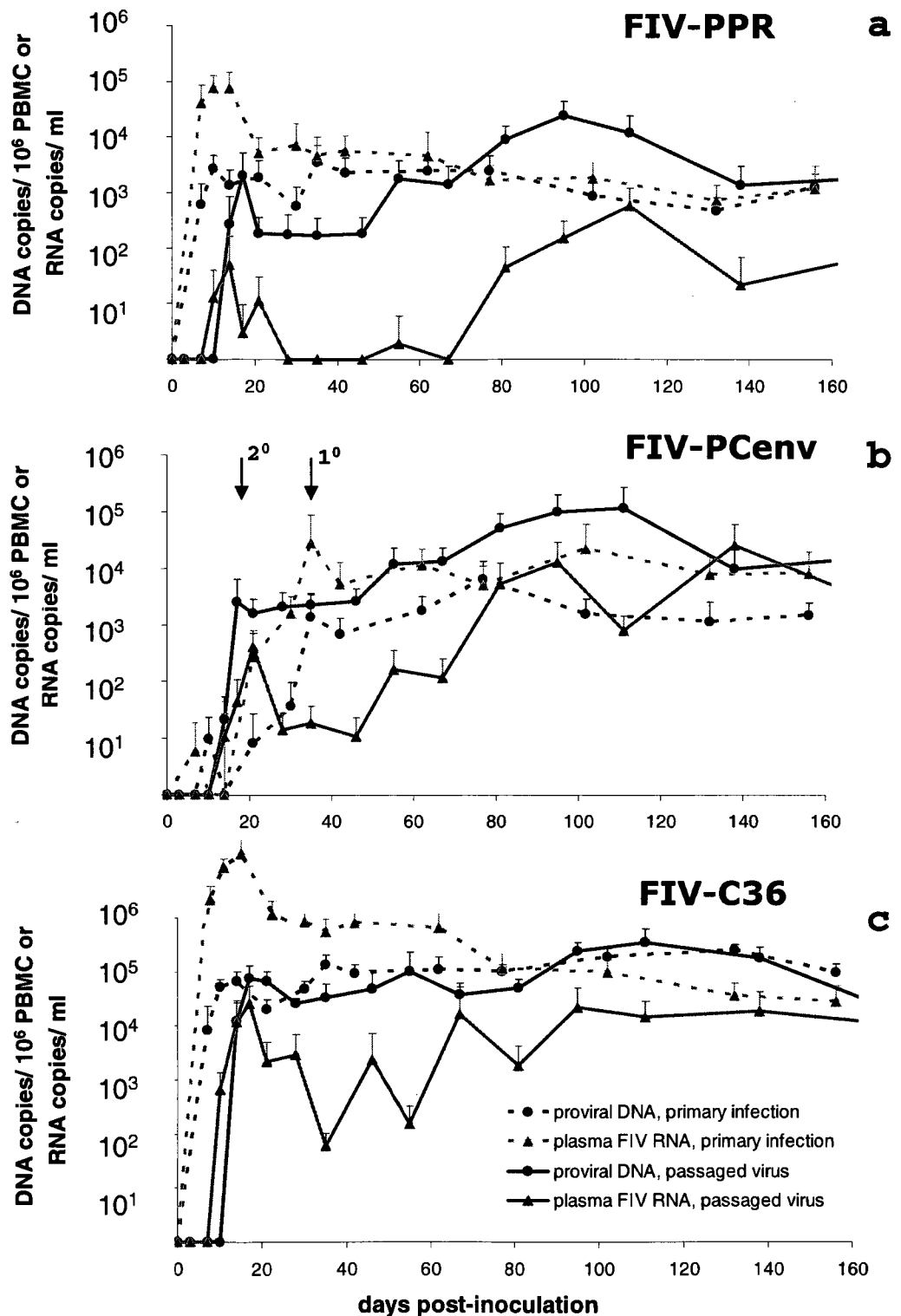


**Figure 2.6:** Comparative replication kinetics during first 160 days of primary viral infection versus passaged FIV-PPR (a), FIV-PCenv (b), and FIV-C36 (c) as previously shown in figures 1.2, 1.3, 2.4, and 2.5. Proviral loads recorded as *gag* equivalents/ 10<sup>6</sup> cells are depicted in green, and circulating virus as RNA genomes/ ml in orange. Red arrows mark the delay in onset of acute viremia in primary versus secondary FIV-PCenv infections.

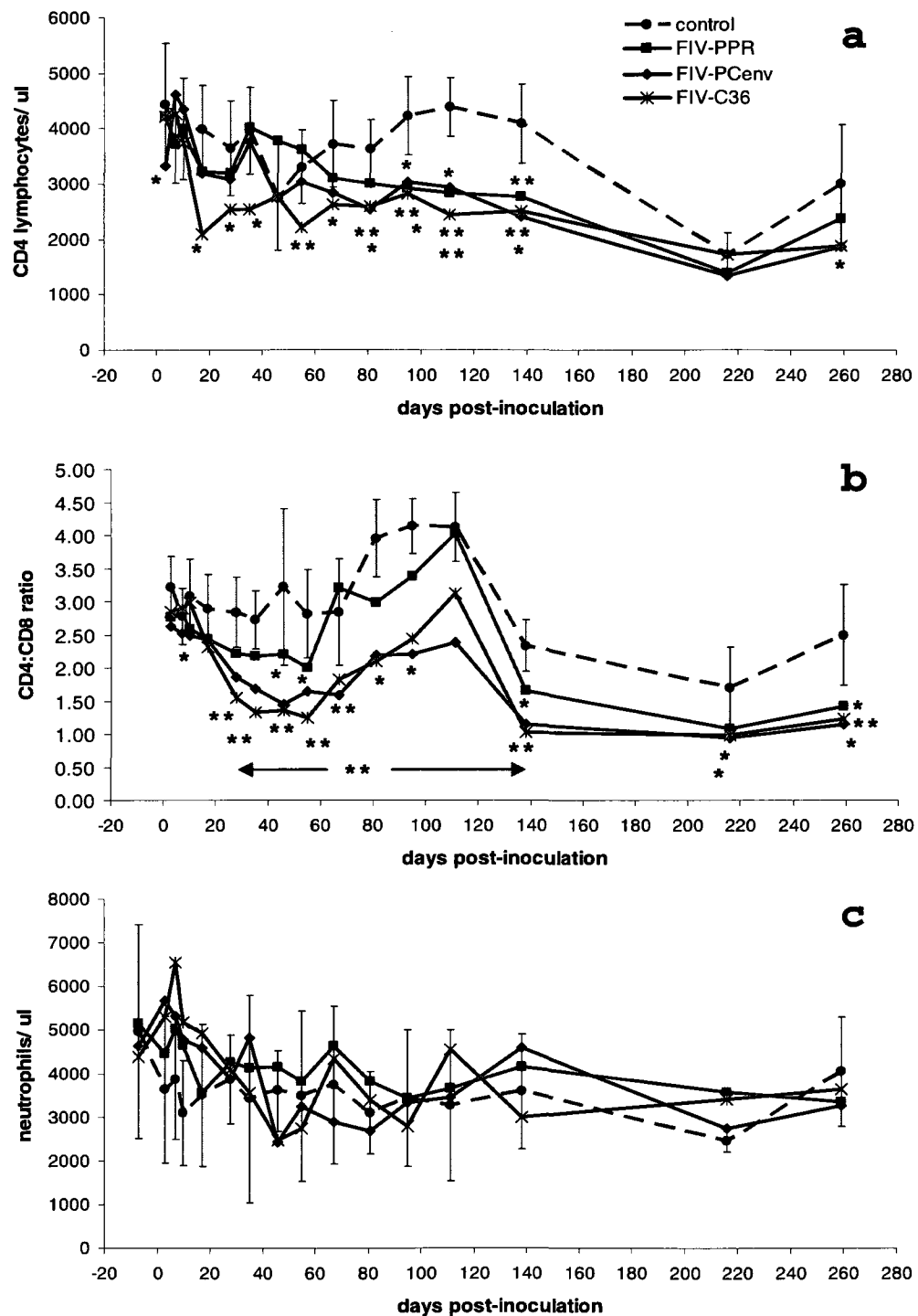


**Figure 2.7:** Timecourse of hematologic changes in domestic cats infected with passaged FIV-PPR, PC-env, and C36. Blood was sampled at various time points over the course of infection. Complete blood counts, differential leukocyte analysis, and CD4<sup>+</sup> and CD8<sup>+</sup> T-lymphocyte percentages in virus-inoculated cats (n=5/group), or sham-inoculated control cats (n=5) were calculated. CD4 counts (shown as number of cells/ $\mu$ l) (a), CD4:CD8 ratios (b), and neutrophil counts (shown as cells/ $\mu$ l) (c) are demonstrated over the course of the study. For ease of viewing, error bars are shown for control group only. Statistically significant values relative to normal control values are indicated by asterisks in same colors used for each viral group (\*,  $P$  between 0.01 and 0.05; \*\*,  $P < 0.01$ ).

differences when compared to non-infected control cats (**Fig 2.7c**). FIV-C36 infection resulted in neutropenia in some individuals starting at day 35 PI, persisting until day 259 PI (data not shown). Likewise, individual FIV-PCenv and FIV-PPR cats, along with one control animal had levels below 2000 at certain sampling points.

## DISCUSSION

We have previously characterized viral kinetics and immunopathology resulting from primary infections with FIV-PCenv, a chimera containing the regulatory elements *vif*, *orfA*, *rev1*, and *env* from a highly virulent clade C strain (FIV-C36) on the background of a moderately virulent clade A strain (FIV-PPR). In preliminary studies described in Chapter One, FIV-PCenv viremia kinetics displayed a lag period during the first month of infection, as well as a delay in classic indicators of immunodeficiency as reflected in drops in CD4<sup>+</sup> T cell and neutrophil counts compared to parental viruses. Eventually, these parameters became intermediate to those of parental viruses. Therefore, we aimed to test the hypothesis that FIV-PCenv genomes were selected and adapted for optimal replication during first-round *in vivo* infections.

Many studies have demonstrated that chimeras generated in the laboratory are typically less virulent than both parental clones (12, 22, 26, 30). This is likely due to the fact that host innate and adaptive immune responses are mounted against viral infection, and successful isolates arise in the face of many factors designed to limit viral success. Despite strong host immunity, a “diversity threshold” model has been proposed in which viral variants with beneficial mutations are able to persist and induce immunodeficiency when the number of diverse quasispecies is high enough (44). This model has been

supported by analysis of *env* evolution during rapid, serial passage of SHIVs in macaques (1). During these *in vivo* passages, infecting virus pool has already overcome the diversity threshold in previous hosts. Thus, upon subsequent rounds of infection in naive hosts, there occurs faster onset of clinical disease accompanied by rapid antibody response and high viral loads (56).

To assess whether chimeric FIV-PCenv experienced mutations during first-round infections that allowed it to display a replication profile intermediate to parental viruses by day 77 PI, we sequenced a total of 4200 nucleotides from the 3' half of the genome. Because this is the region hypothesized to contain virulence factors, and due to the hypervariable nature of *env*, sequencing here was undertaken first. It is also possible that the FIV-C36 portion of FIV-PCenv influenced changes within the 5' FIV-PPR half of the chimera, leading to its replicative capacity.

The Rev protein of FIV-PCenv is expressed via a multiply-spliced transcript containing two exons (10, 72); *rev1* is derived from FIV-C36, while *rev2* is coded on the FIV-PPR background of the chimera. Upon sequencing of provirus from an infected cat, the FIV-C36 portion of FIV-PCenv revealed an A→G mutation within the RRE which reverted the predicted secondary structure from that of FIV-C36 back to FIV-PPR based on published parental sequences. Twenty-five of the 147 nucleotides of the FIV-PCenv RRE are of FIV-PPR origin as highlighted in figure 2.3; however, only 3 of these 25 differ between FIV-PPR and FIV-C36. These differences are not substantive enough to alter the secondary structure in this region as predicted by algorithms used by 'RNAfold', discounting a direct role for RRE chimerism in manifesting the observed change in virus isolated on day 77 PI compared to inoculum. Since no mutations were detected in the

chimeric Rev protein of FIV-PCenv, we can postulate that selection of an RRE mutant may have been essential for proper function of the chimeric Rev protein. Over time, the replicative success of this mutant may have resulted in the emergence of a more fit quasispecies which had the potential to more actively infect PBMC and bone marrow reservoirs of circulating virus, ultimately leading to the hematologic consequences noted during *in vivo* trials.

This provides preliminary data that selection of this variant was perhaps necessary for optimal replication function of the chimera. The predicted changes in secondary structure could have implications for the efficiency of Rev interactions with the RRE on unspliced and singly-spliced viral transcripts, and may help explain the intermediate phenotype seen during FIV-PCenv infections. Future studies would include obtaining additional sequences of this region from other cats infected with FIV-PCenv, and resequencing the inoculum stock to rule out that these changes occurred during *in vitro* amplification prior to cat inoculations. It would also be worthy to obtain direct sequence at various time points PI for inclusion in a more comprehensive data set cataloguing molecular changes correlating to disease phenotype.

While plasma viremia in FIV-PCenv cats mirrored that of FIV-C36 one and a half months into primary infection, proviral copy numbers in PBMC or bone marrow of cats infected with the chimera never reached the values of FIV-C36. However, *in vivo* passage of FIV-PCenv resulted in viral RNA and DNA copy numbers equal to those measured for passaged FIV-C36 by day 81 PI. Moreover, FIV-PCenv provirus values were one order of magnitude higher during second passage in domestic cats, suggesting that either the initial replication competent FIV-PCenv inoculum dose was higher during

second round infection, or that progressive replication enhancement continued during second passage. These increases in FIV-PCenv viremia compared to parental FIVs within each study and to itself during consecutive rounds of infections support the notion that after a period of adaptation, molecular determinants from FIV-C36 in some way confer enhanced virulence to FIV-PCenv.

Although slight neutropenia was observed in three FIV-C36 cats between days 35 and 259 PI, mean neutrophil levels never significantly varied from those of mock-infected controls. Statistically, this may have been due to control cats that had low neutrophil counts at seven time points; factors such as cage environment, allergies, or stress can contribute to variability in hematology parameters (64). One FIV-PCenv cat also experienced neutropenia starting at day 46 PI, rebounding by day 95 PI. None of these effects, however, resembled the marked neutropenia observed during first-round infections with FIV-C36 or FIV-PCenv. The more dramatic neutrophil declines observed during primary infections with FIV-C36 and FIV-PCenv may indicate that the biological inoculum (pooled plasma) used for *in vivo* passage was a lower titer, or contained more varied viral quasispecies.

Similar to primary infections, CD4<sup>+</sup> T-cell declines were observed starting on day 17 PI in FIV-C36 cats and persisting until day 138 PI. Statistically significant differences in CD4<sup>+</sup> T-cell counts of the FIV-PCenv group compared to controls began on day 63 PI. Previous infections with this chimera resulted in a rebound in CD4 levels compared to controls. Conversely, during second-round infection, *P* values remained below 0.01 through day 138 PI. The FIV-PPR group also had significant differences compared to

controls between days 95 and 138 PI, strengthening the hypothesis that viral passage results in enhanced virulence.

FIV-PCenv contains large portions of two separately evolved genomes. Therefore, FIV-C36 and FIV-PPR elements must act in concert with each other during multiple phases of the viral lifecycle. Transcription, nuclear export of mRNAs, translation and polypeptide cleavage, viral assembly and maturation, envelope recognition and binding of naïve cells, nucleocapsid uncoating, reverse transcription, formation of pre-integration complexes, and proviral integration are some major events which are certainly affected. Such widespread downstream effects of a chimeric genome could hamper the ability of FIV-PCenv to fully mimic FIV-C36. For example, in both primary and passaged infections, initial spikes in FIV-C36 viremia were at least two orders of magnitude greater than in FIV-PCenv. The findings presented here indicate a role for FIV-C36 elements in FIV-PCenv pathogenesis when compared to FIV-PPR infections, but genetic manipulation is potentially responsible for the intermediate phenotype of FIV-PCenv. To investigate whether a particular genomic element is responsible for the heightened virulence of FIV-C36, it will be necessary to perform infections using chimeras which express just one FIV-C36 gene on the FIV-PPR background. Experiments with FIV accessory-gene chimeras in which smaller regions of the genome have been swapped may provide insight using a less invasively-engineered molecular construct.

## CHAPTER THREE

### Generation of FIV Accessory-Gene Chimeras

#### INTRODUCTION

Infections of the domestic cat with molecular clones representing clade C and clade A FIV isolates (FIV-C36 and FIV-PPR, respectively), recapitulate the phenotypes of parental viruses (11, 66). Chapters One and Two describe the *in vivo* kinetics of FIV-PCenv, a chimera containing the 3' half of FIV-C36 including *vif*, *orfA*, *rev1*, and *env*, on the FIV-PPR background. FIV-PCenv demonstrated intermediate, although delayed, viral loads and hematological pathology during primary infection (12). We have shown that passage of FIV-PCenv into naïve cats results in higher viral loads similar to those observed during parental FIV-C36 infections, which are not delayed compared to parental constructs (Chapter Two). Results from experiments with clade A/C chimeric FIV-PCenv suggest that elements from the 3' half of the genome may contribute to the heightened virulence observed during infections with clade C FIVs. Furthermore, during *in vivo* passage of the virus, FIV-PCenv viremia rates were no longer delayed, and viral load levels markedly increased, suggesting viral adaptation via passage through cats.

Gag structural proteins are expressed from the 5' half of the FIV genome and include matrix, capsid, and nucleocapsid. Reverse transcriptase, integrase, protease, and dUTPase enzymes are expressed from *pol*. FIV-PPR and FIV-C36 *gag* and *pol* are more conserved at the nucleotide level than *env* and other 3' counterparts (Table 3.1). Minor differences in nucleotide homology can result in more pronounced changes in amino acid coding sequence as demonstrated in Figure 3.1 for accessory proteins OrfA and Rev. Of

	nucleotide positions	# bases	% nt identity
entire genome	1-9467	9467	83
5' half	354-5248	4894	85
5' LTR	1-354	354	84
<i>gag</i>	633-1986	1353	85
<i>pol</i>	2256-5249	2993	85
3' half	5205-9210	4005	81
<i>env</i>	6271-8836	2565	81
<i>vif</i>	5205-5994	789	83
<i>orfA</i>	5997-6234	237	75
<i>rev1</i>	6271-6512	241	81
<i>rev2</i>	8943-9164	221	88
RRE	8784-8931	147	92
3' LTR	9210-9467	257	89

**Table 3.1:** Nucleotide homology between regions of FIV-PPR and FIV-C36 based on NCBI Blast results. 5' half represented from the end of 5' LTR to end of *pol* gene; 3' half by start of *vif* to start of 3' LTR.

**Vif (263aa) 84.4% identity**

GESQNPALFL	KGMSEEDWQV	SKGLFAVLQG	GVHSAMLYIS	FIV-C36
RESQNPALFL	KGMSDEDWQV	SRRLFAVLQG	GVYNAMLYIS	FIV-PPR
ELPEMEKEQY	KKEFKRLLD	KETGFIRRLR	KAEGIKWSFH	FIV-C36
RLPQDEREKY	KKDFKRLLD	TETGFIKRLR	KAEGIKWSFH	FIV-PPR
TRDYVMGYVK	ELVAGSSTPD	SLRLYIYISN	PLWHGKYRPG	FIV-C36
TRDYHVGIVR	EMVAGPTTPH	SLRLYVYISN	PLWHSQYRPG	FIV-PPR
LKNFNKEWPF	VNMWIKTGFM	WDDIEKQKIC	VGGEISPGWG	FIV-C36
LVNFNKEWPF	VNLWIKTGFM	WDDIEKQNIC	IGGEVSPGWG	FIV-PPR
PGMVGIAIKA	FSCGERKIEA	TPVMIIREEI	DPKKWCGDCW	FIV-C36
PGMIGIAIKA	FSCGERKIEA	TPVMIIRGEI	NPKKWCGDCW	FIV-PPR
NLMCLRNSPP	GTLQRLAMLA	CGRKAKCWRG	CCNQRVFSY	FIV-C36
NLMCLRNSPP	ETLQRLAMLA	CGVQAKSWRG	CCNQRVFSY	FIV-PPR
RTPADLEVIQ	YKPGWNLLWL	GEL		FIV-C36
RTPADLEVIQ	SKPGWCMLWR	GKL		FIV-PPR

**ORFA (78aa) 65.4% identity**

MEEIIPLFNK	ATDKLGQEA	IRLFVLAHQI	ERDKFIRLLH	FIV-C36
MEVIRI-FNK	VAERLDKEA	IRIFVLAHQI	ERDKLIRLLQ	FIV-PPR
LLIWRDRFKV	PNPRGCLCWW	CCKLYYWQLO	STLSISSA	FIV-C36
GLLWRLRFRK	PKSKDCLCWF	CCRLYYWQLO	STLSIDTA	FIV-PPR

**Rev (154aa) 70.8% identity**

MAEGFCQNRQ	WIGPEEAEEL	LDFDIATQVS	EEGPLNPGIN	FIV-C36
MAEGFAANRQ	WIGPEEAEEL	LDFDKATQMN	EEGPLNPGVN	FIV-PPR
PFRQPGLTDG	EKEEYCKILQ	PRLQALREEY	KEGSLNSECA	FIV-C36
PFRVPAVTEA	DKQEYCKILQ	PRLQEIIRNEI	QEVKLEEGNA	FIV-PPR
AVL GKRKRQR	RRRKKKAFKR	MMTDLEDRF-	KLFGSPLTDE	FIV-C36
GKM -KKRQR	RRRKKKAFKK	MMTDLEDRFR	KLFGSPSKDE	FIV-PPR
-AADAKDE-P	PKKEKRDWE	DYWDPEIEEK	MLMD	FIV-C36
YTEIEIEEDP	PKKEKRDWD	EYWDPEEIER	MLMD	FIV-PPR

**Figure 3.1:** Amino acid sequences of the accessory proteins Vif, OrfA, and Rev from the highly pathogenic molecular clone FIV-C36 (clade C) aligned with those of the less pathogenic FIV-PPR (clade A). Yellow highlight= prolines in C36 OrfA not present in PPR. Red line denotes separation of Rev exons.

potential importance are two prolines found in FIV-C36 OrfA that are lacking in the FIV-PPR protein; due to the ring-structure of proline, incorporation of this amino acid introduces a kink or breakage within the  $\alpha$ -helical secondary structure of a protein that could significantly augment the functional properties of this isolate.

Evidence thus far points to a vital role for FIV regulatory proteins in the initiation and maintenance of chronic viral infection. Mutant FIVs in which these genes have been disrupted are not able to attain wild-type replication levels (23, 24, 35, 43, 59, 71), and are restricted to certain cell types (24, 53, 74). The exact nature of the functions of these proteins and their contribution to viral pathogenicity has yet to be elucidated; therefore, they remain an important target of continued investigation.

To test the hypothesis that FIV-C36 accessory genes *vif* and *orfA* are elements that confer enhanced pathogenic potential to clade A/C chimeric FIV-PCenv, we used overlapping PCR, or PCR-driven overlap extension (20) (**Fig 3.2**), to generate chimeras with FIV-C36 accessory genes on an FIV-PPR backbone. Here, we describe the production of replication-competent molecular constructs designated as FIV-PCvif, FIV-PCvif/orfA, and FIV-PCorfA (**Fig 3.3**), and initial efforts at production of infectious virus using these clones.

In an attempt to define molecular determinants of FIV pathogenesis, we assessed the capacity of parental and *vif/orfA* gene chimeras to infect the feline T-cell line MYA-1 and primary feline PBMCs. Replication capacity was determined using multiple assays measuring different aspects of viral production. Replicative kinetics of FIV-PCvif/orfA evaluating both capsid antigen and viral RNA production demonstrated that FIV-C36 Vif and OrfA, when expressed in combination with backbone elements of FIV-PPR, confer

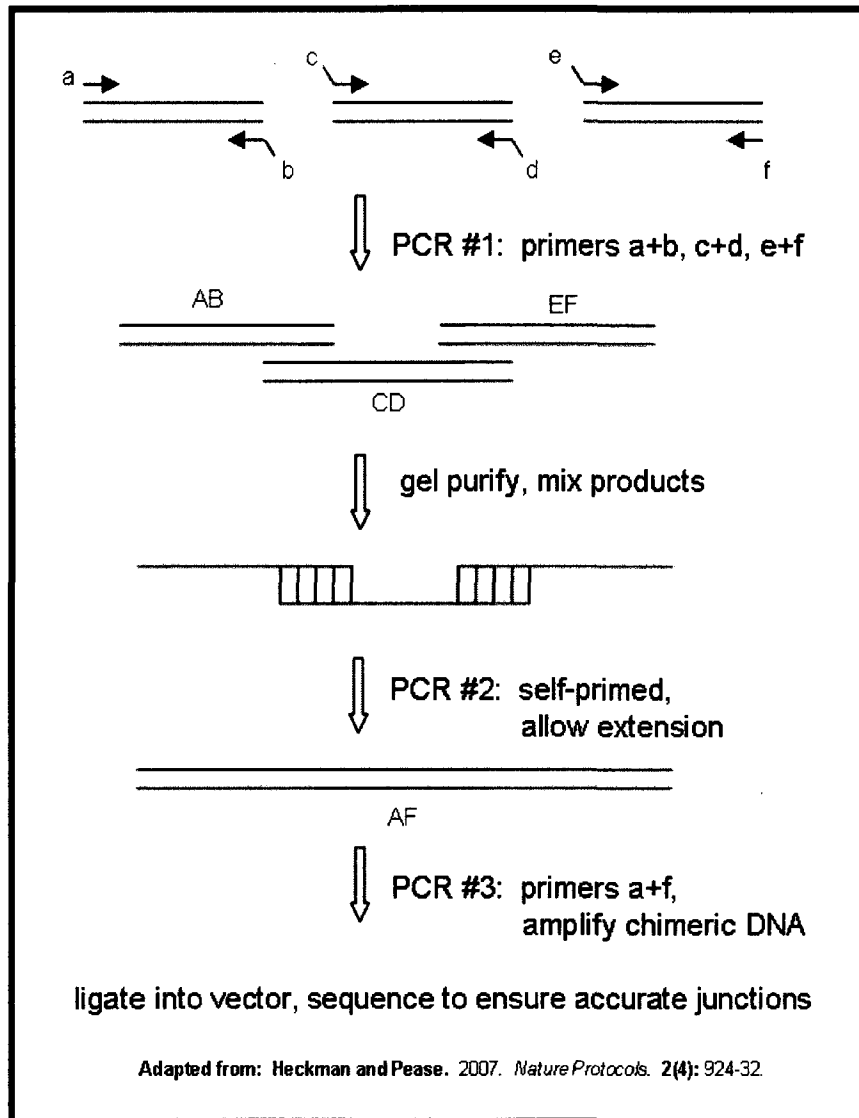


**Figure 3.2:** Primers are designed to include tail regions on the products which match sequence from the opposing virus. Chimeric AF fragments are generated by mixing the products of reactions AB, CD, and EF in a self-primed, overlapping PCR reaction. This product is then amplified using AF primer pair to yield sufficient amounts for ligation into parental plasmid.

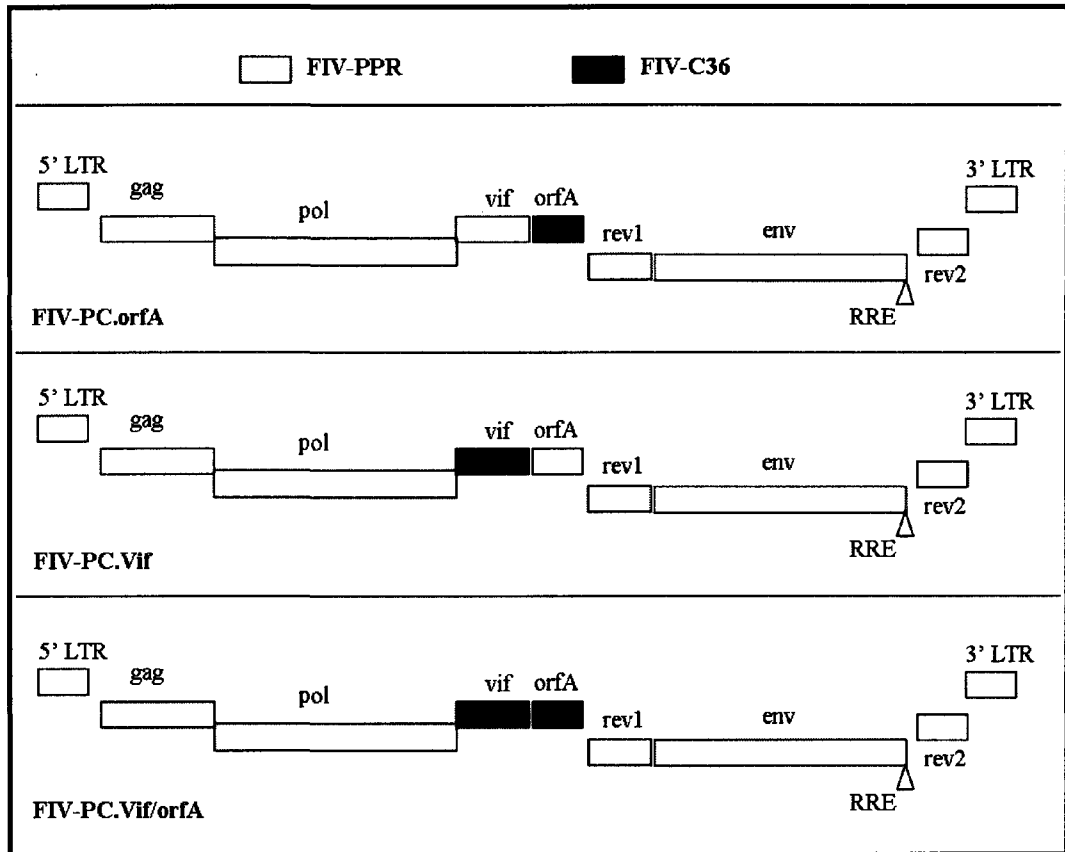


**Figure 3.3:** Clade A/C FIV accessory-gene chimeras. Clade C FIV-C36 *orfA* and *vif* genes (depicted in black) were exchanged with those of clade A FIV-PPR using PCR-driven overlap extension.

replication properties similar to parental FIV-C36 in MYA-1 cells. In contrast, FIV-PCvif/orfA infections of primary feline PBMC yielded levels lower than those of both parental viruses.

Similar studies using chimeric viruses expressing only one or the other of these proteins from FIV-C36 will help to elucidate how these constituents affect viral replication independent from one another—and to ultimately elucidate mechanisms underlying the high pathogenicity of FIV-C36.

## **MATERIALS AND METHODS**

**Generation of constructs.** We used plasmids containing full-length parental constructs FIV-PPR and FIV-C36 as template to generate fragments AB (PPR), CD (C36), and EF (PPR) using Platinum® Pfx DNA high-fidelity polymerase (Invitrogen, Carlsbad, CA). Reaction conditions were as follows: 30 cycles of denaturation at 94°C for 15 sec., annealing at 55°C for 30 sec., and extension at 68°C for 1 min. Products were separated on an agarose gel, stained with crystal violet, and extracted using the QIAquick gel extraction and purification kit (Qiagen, Valencia, CA). After self-primed overlapping reaction between fragments AB, CD, and EF, we amplified full-length chimeric AF product with primers A and F to generate sufficient amounts for crystal violet gel extraction and ligation into pFIV-PPR. Self-primed and AF amplification reaction conditions were as follows: 30 cycles of denaturation at 94°C for 15 sec., annealing at 58°C for 30 sec., and extension at 68°C for 2 min.

Restriction endonuclease digestions of AF fragments using *EcoRV*, *Bsu36I*, and *BclI*, and ligations using T4 DNA ligase, were performed according to manufacturer's

specifications (New England Biolabs, Ipswich, MA). All chimeric clones were transformed in MAX Efficiency® Stbl2™ competent *E. coli* (Invitrogen) and grown at 30°C in order to avoid instability and recombination of lentiviral sequences. All constructs were validated by restriction enzyme analysis and PCR using primer sets AD, CD, and CF (Fig 3.6). Clones were directly sequenced by Laragen, Inc. (Los Angeles, CA), using Sequencher™ software (Gene Codes Corporation) to verify PPR/C36 junctions and re-establishment of restriction sites.

**Primers.** Primers A and F, specific for pFIV-PPR, were used for the generation of all chimeras and the sequences are as follows: A(f)=TGTTGC CTAAAGGACATTGG and F(r)=TTTGGTATCTCCGGGTCTTG. Primers B-E and B.2-E.2 were designed to ensure accurate junctions between parental constructs and are as follows: FIV-PCvif: B(f)=GTTCTGGGACTCTCCTTACGTGTCTCCT AGG, C(r)=CCTAGGAGACAC GTAAGGAGAGTCCCAGAAC, D(f)=CGTATTACTTCCATTCATAGCTCTCCTAA CCATAGC, E(r)=GCTATGGTTAGGAGAGCTATGAAT GGAAGTAATACG; FIV-PCorfA: B.2(f)=AATTATCTCTTCCATTCACAGTT TTCCTCG, C.2(r)=CGAGGAA AACTGTGAATGGAAGAGATAATT, D.2(f)=GCTGCA AACCTTCTGCCATATTT ATTGATGTAGATG, E.2(r)=CATCTACATCAATAAATATGGCAGAAGGGTTTGC AGC. Underlined regions indicate reverse complement sequences specific to FIV-C36. Based on the 5'-3' arrangement of *vif* and *orfA* on the FIV genome, primers B, C, D.2, and E.2 were thus used for construction of FIV-PCvif/orfA. A schematic of primer touchdown and predicted AB, CD, and EF fragment sizes for each construct is presented in Figure 3.4.

**Overlapping PCR methods development.** Choice of the internal primers B/C and D/E for each construct was restricted to areas overlapping the start and end of accessory gene open-reading frames. Using online resources (Oligo Calc: oligonucleotide properties calculator. Kibbe WA. 2007), primers were evaluated for self-complimentarity. Due to multiple predictions for self-dimerization and hairpin formation, an additional set of D/E primers complimentary for a region 20 nucleotides downstream from the exact gene/non-coding junction was tested during FIV-PCorFA construction. This second primer set was ultimately used for chimera construction, as the primers specific for the exact junction between *orfA* and 3' non-coding sequence were unable to amplify product and formed dimers as visualized in an agarose gel (data not shown). Design of primers A and F was less restricted as sequence representing a specific gene transition was not required, but it was necessary to design these primers outside of restriction endonuclease recognition sites used for insertion of AF fragments into parental plasmid. In addition, to avoid pitfalls involved in cloning larger fragments, external primers were designed to minimize amplified product lengths.

The restriction enzyme *BclI* is restricted by the action of DNA methylation at the N<sup>6</sup> position of the adenine in the sequence GATC by most strains of *E. coli* (*dam* methylation). Therefore, it was necessary to grow pFIV-PPR in *E. coli* that had a null mutation for this gene (*dam*<sup>-</sup>). Because these bacteria are more prone to DNA recombination, growth conditions were controlled to ensure sufficient plasmid yield while minimizing the opportunity for FIV LTR-mediated recombination of the full-length lentiviral sequence.

Ultraviolet irradiation of DNA PCR fragments can result in strand nicks or breaks, ultimately leading to mutation during DNA repair. To avoid this, we used agarose gels stained with crystal violet which allowed visualization of bands without application of UV light when fragments were to be extracted for use in subsequent ligation reactions.

**Cell culture preparations.** Crandell feline kidney cells (CrFK) (8) were grown at 37° C in 5% CO<sub>2</sub> in Dulbecco's Modified Eagle Medium (DMEM, Gibco, Carlsbad, CA) supplemented with 10% fetal bovine serum (FBS) and 1% penicillin-streptomycin (P/S) (10,000 U(P) or µg(S)/ ml). We purified PBMCs on a Histopaque-1077 (Sigma, St. Louis, MO) gradient, washed them in phosphate-buffered saline (PBS), and cultured them immediately for up to 14 days. Primary feline PBMC as well as the feline T-lymphoblastoid cell line, MYA-1 (39), were grown in RPMI media (Gibco), supplemented with the following: 20% FBS, 10% D-glucose, 1% P/S, 1% Na-bicarbonate, 1% non-essential amino acids, 1% Na-pyruvate, 0.1% β-2-mercaptoethanol. For stimulation, 10 ng/ml human recombinant interleukin-2 (Chemicon International, Temecula, CA) was added to T-cell cultures.

**Transfections and generation of viral stocks.** CrFK cells ( $3.6 \times 10^5$ ) were plated in 6 well (35 mm) plates, allowed to attach overnight, and transfected with 2 µg of plasmid DNA containing full-length chimeric FIVs using Fugene™6 (Roche, Nutley, NJ) reagent according to manufacturer's instructions. After incubating cells for 48 hours, transfection supernatant was assayed by RT-PCR and ELISA to confirm presence of

virus. Virus-positive CrFK transfection supernatant was used to infect MYA-1 cells for generation of virus stocks. MYA-1 supernatant was collected on day 14, and assayed by RT-PCR. CT values were used to determine viral particle number for subsequent culture experiments using different multiplicities of infection (MOI).

**Assessment of *in vitro* infection kinetics.** Based on particle numbers determined by real-time PCR, we infected in triplicate  $1 \times 10^6$ / ml PBMC or MYA-1 cells with a normalized volume of FIV-PCvif/orfA virus stock at MOI of 0.1 and 0.01. Infections with MYA-1 generated parental stocks (FIV-PPR and FIV-C36) were performed in tandem. All cultures were incubated at 37° C with 5% CO<sub>2</sub> in 24-well plates. Supernatant was harvested on days 7 and 14 for viral detection by p25 capsid antigen-capture ELISA, RT-PCR to quantify viral genomes (Methods described in Chapters One and Two), or RT-assay in order to assess replication kinetics of similar input viruses on primary cells or MYA-1 feline T-cell line. Cell pellets were retained for detection of integrated provirus.

**Antigen capture ELISA.** Monoclonal anti-FIV antibody (mu51G11.1) was applied to 96-well microtiter plates at 1125 ng per well in 0.1 M carbonate buffer (pH 7.2). We incubated plates overnight at 4°C, washed, and blocked with buffer containing 2% bovine serum albumin (BSA). To bind FIV p25 antigen, we added 50 µl sample to 100 µl enzyme-linked immunosorbent assay (ELISA) buffer (TEN; 2% BSA, 5% FBS, 0.5% Triton X-100) per well and incubated at room temperature for 2 h. Plates were washed with TEN (50mM Tris, 0.1mM EDTA, 150mM NaCl, 50mM HCl, pH 7.2)

containing 2% Tween-20 (polyoxyethelene sorbitan monolaurate). Serum from a persistently FIV-infected domestic cat diluted 1:200 in ELISA buffer was applied and incubated for 45 min. To detect bound antibody, we used peroxidase-labeled goat anti-feline immunoglobulin G (IgG) (Kirkegaard & Perry Laboratories, Inc., Gaithersburg, MD) diluted in ELISA buffer containing 5% mouse serum. TMB (3,3',5,5'-tetramethylbenzidine) substrate (Kirkegaard & Perry Laboratories, Inc.) was applied to detect colorimetric reactions. Reactions were stopped with 2.5M H<sub>2</sub>SO<sub>4</sub> and plates were read at an absorbance of 450 nm.

**RT-assay.** To detect reverse-transcriptase (RT) activity in infected cell supernatants, we used a method derived from (18, 76). Fifteen µl previously frozen supernatant was incubated with 50 µl master mix containing 1 M Tris-HCl (pH 7.8), 3 M KCl, 0.1 M dithiothreitol, 0.15 M MgCl<sub>2</sub>, 0.025 U of poly(rA-dT)<sub>12-18</sub>, 2% NaPO<sub>4</sub>, 10 mM EGTA, and 1.1 µCi of [<sup>32</sup>P]dTTP at 37°C for 2 h. Next, 2.5 µl each sample was spotted onto Whatman filter paper, allowed to dry, and washed five times with a solution of 0.15 M NaCl and 15 mM sodium citrate. After one final 95% ethanol wash, filters were allowed to dry and radioactivity was recorded as counts per minute using a 1450 Microbeta Plus liquid scintillation counter (Wallac/ PerkinElmer, Waltham, MA).

## RESULTS

We used primer pairs to amplify the FIV-C36 accessory genes *vif*, *orfA*, or *vif/orfA* in tandem. Using two additional primer pairs, we amplified regions from FIV-PPR which flank FIV-C36 *vif* and *orfA*. We designed all three primer pairs so that the

resulting amplicons contained ends with sequences complimentary to the opposite virus. When we mixed the three products with dNTPs and polymerase, complimentary regions between FIV-PPR and FIV-C36 allowed for a self-primed PCR reaction, producing chimeric overlapping-PCR products. Next, using restriction enzymes, we inserted these products into the backbone of FIV-PPR, generating FIV-PCvif, FIV-PCorfA, and FIV-PCvif/orfA (**Fig 3.3**).

***Amplification of PPR and C36 PCR products.*** For each chimeric construct, we designed primers to amplify products AB and EF (**Fig 3.4**), upstream (AB) and downstream (EF) from accessory gene sequences. We used plasmid DNA (pFIV-PPR), containing full-length FIV-PPR, as template. A third product, CD (**Fig 3.4**), representing *vif* and *orfA* regions, was generated by amplification from plasmid containing full-length FIV-C36 (pFIV-C36). Primer positions on the FIV genome and expected sizes of PCR products are shown in figure 3.5.

During the overlapping-PCR reaction, denatured strands of products AB, CD, and EF were able to hybridize at the complementary regions designed on internal primers B-E due to inclusion of a sequence tag representing sequence from the complimentary DNA strand. Since product from the self-primed, overlapping-PCR reaction is minimal and barely visible on an agarose gel, it was used as template to amplify sufficient amounts of AF products by addition of primers A and F to another PCR reaction (**Figs 3.2 and 3.4**). AF products were screened via PCR with primer sets AD, CD, and CF (**Fig 3.6**) prior to endonuclease digestion and insertion back into pFIV-PPR.

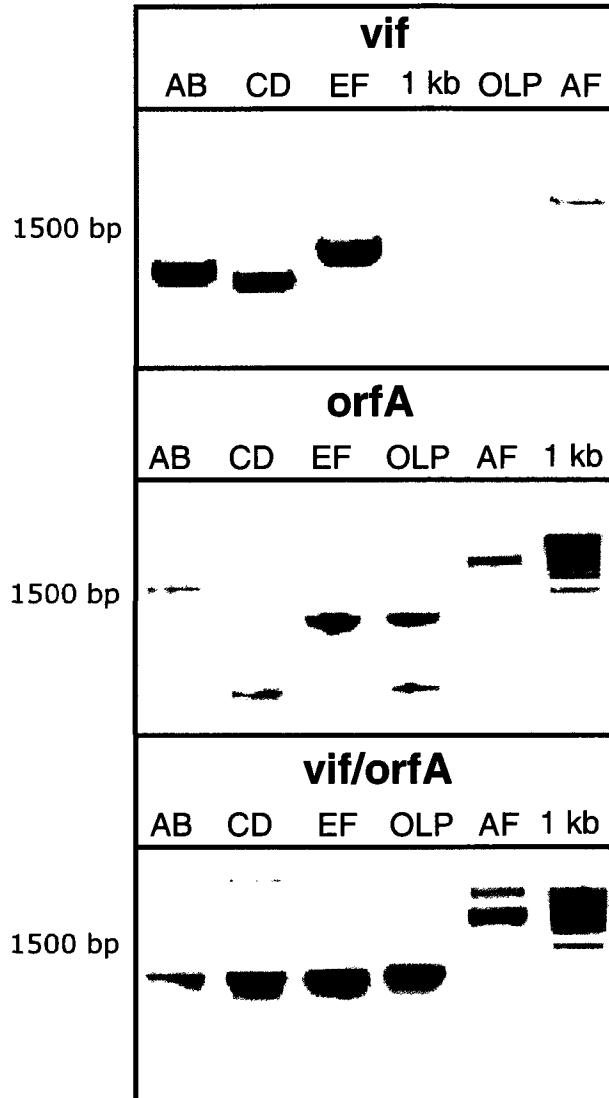


**Figure 3.4:** Generation of fragments for use in PCR-driven overlap extension using primer pairs AB, CD, and EF. OLP= product formed during self-primed, overlapping PCR reaction. AF= amplified OLP used for ligation into pFIV-PPR to yield chimeric constructs pFIV-PCvif, pFIV-PCorfA, and pFIV-PCvif/orfA.

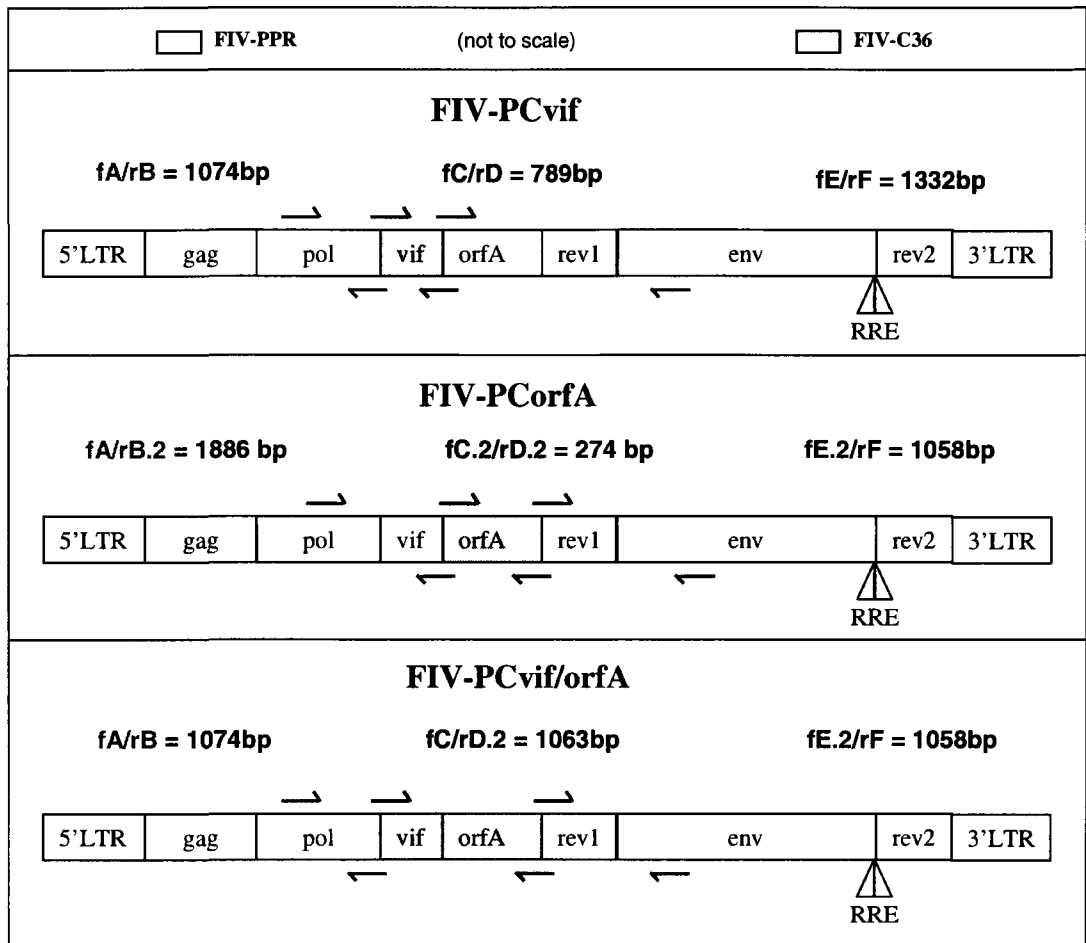


**Figure 3.5:** Schematic showing oligonucleotide touchdown sites and predicted product sizes using primer pairs AB and EF to amplify flanking regions from pFIV-PPR (white), and primer pair CD to amplify accessory gene sequences from pFIV-C36 (gray).

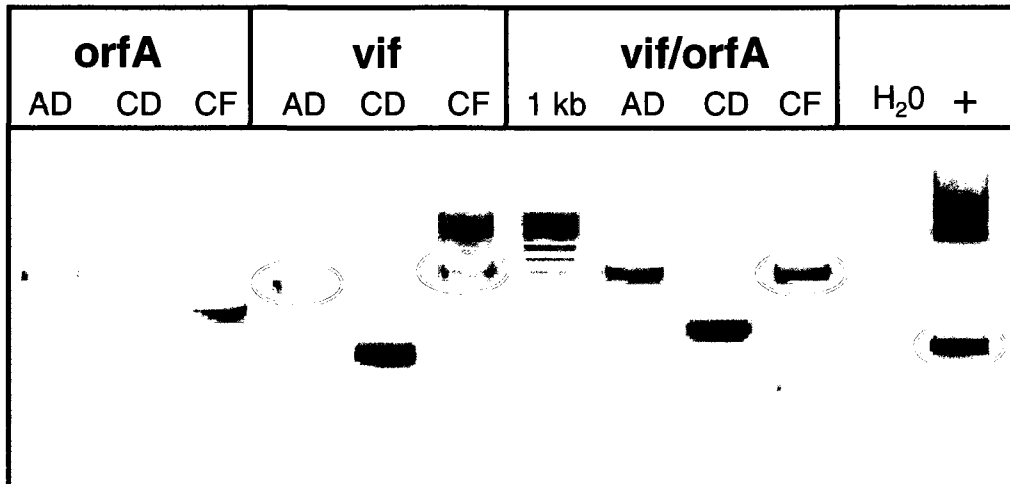


**Figure 3.6:** PCR confirmation of fragments generated via PCR-driven overlap extension. Chimeric AF fragments orfA, vif, or vif/orfA were tested with primer pairs AD, CD, and CF. For lanes in which multiple bands are present, predicted products are circled in red.

**Chimera construction.** External oligonucleotides A and F were designed outside of the restriction endonuclease recognition sites being used to insert chimeric DNAs into parental pFIV-PPR (**Fig 3.7**). To generate FIV-PCvif and FIV-PCvif/orfA fragments (3027 base-pairs) for use in ligation, we used *EcoRV* and *BclI* to digest overlapping-PCR AF products. We digested FIV-PCorfA AF products using *BclI* and *Bsu36I*, yielding 1918 base-pair ligation fragments. Transformants were screened via PCR, restriction digest, and direct sequencing to ensure correct junctions between FIV-PPR and FIV-C36 genomes.

One clone for each chimera was chosen based on accurate sequences of total chimeric region, including primer junctions and restriction sites used for construct insertion. Representative alignments of chimera clones with proposed sequence derived from published FIV-PPR and FIV-C36 electronic sequences are shown in Figure 3.8. All junctions between FIV-C36 genes and FIV-PPR backbone were highly specific for *vif* and *orfA* open-reading-frames. Primers designed at the exact 3' junction of *orfA* yielded primer dimers, coupled with an unsuccessful PCR. Therefore, an additional set of D/E primers that annealed 20 nucleotides downstream was used. This resulted in inclusion of non-coding FIV-C36 DNA in FIV-PCvif/orfA and FIV-PCorfA that had no effect on amino acid sequence.

**Transfections and generation of viral stocks.** Cell-free supernatant from CrFK cells transfected with plasmids containing full-length FIV-PPR/C36 chimeras were positive for FIV p25 antigen and RNA genomes (data not shown). Transfection supernatant was used for small-scale infections of the MYA-1 feline T-cell line, and all

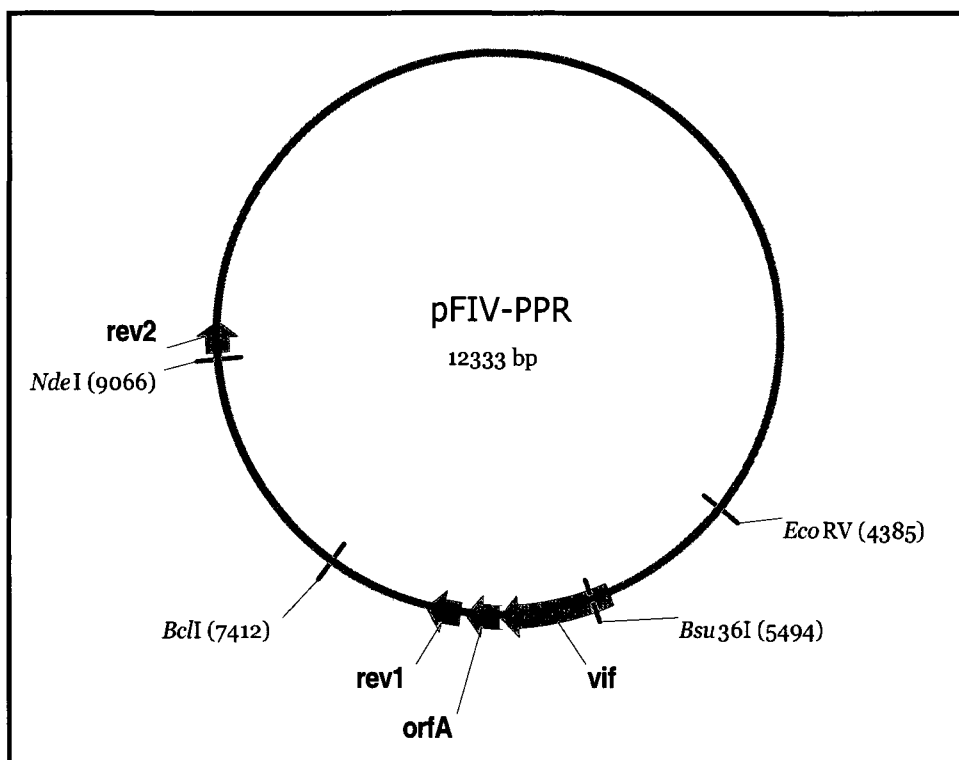


**Figure 3.7:** Representation of plasmid containing full-length FIV-PPR. Open-reading frames encoding the accessory gene products Vif, OrfA, and Rev are shown in orange. BclI and Bsu36I restriction endonuclease recognition sites were used to construct pFIV-PCorfA, while BclI and EcoRV sites were used to construct pFIV-PCvif and pFIV-PCvif/orfA.

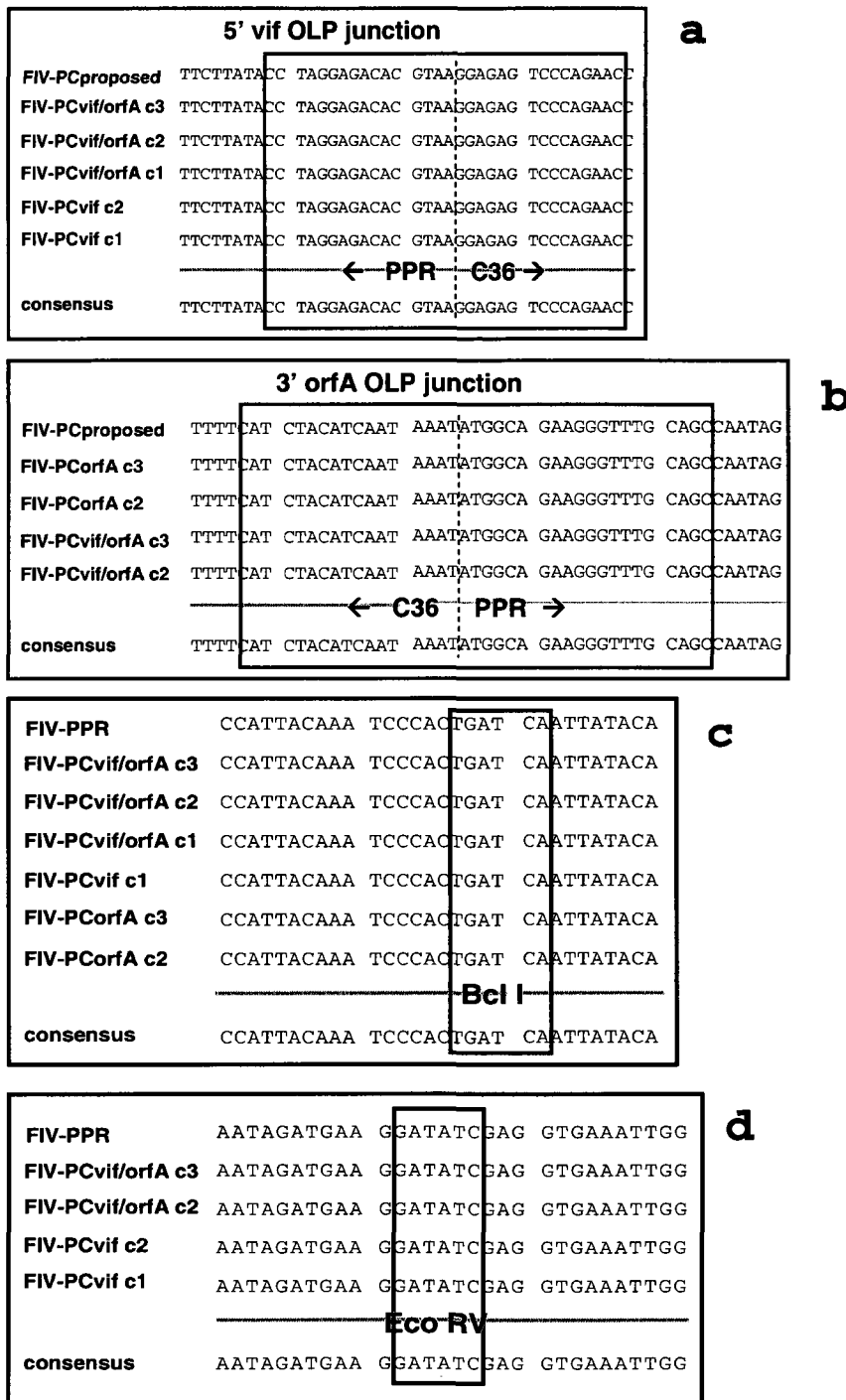


**Figure 3.8:** Nucleotide sequence alignments chimeric junctions of FIV-PCvif, FIV-PCorfA, and FIV-PCvif/orfA clones compared to electronic sequence of proposed constructs (a and b). Verification of re-established restriction endonuclease recognition sites in chimeras versus parental FIV-PPR into which chimeric fragments were backcloned (c and d).

supernatants demonstrated RT-activity with signals above background as measured by incorporation of radio-labeled thymidine and recorded as counts per minute, confirming generation of replication-competent virions from transfected plasmids containing full-length chimeric FIV-PCorfA, FIV-PCvif/orfA, and FIV-PCvif (**Fig 3.9**).

Large-scale viral stock was generated for FIV-PCvif/orfA by infection of MYA-1 cells with CrFK transfection supernatant. To confirm presence of virus, supernatants collected 7 and 14 days PI were evaluated by ELISA as described above. Based on ELISA values that exceeded both negative controls and day 7 values, day 14 PI supernatant was harvested and frozen in 1 ml aliquots as stock to use in infectivity studies.

***in vitro replication kinetics of FIV accessory-gene chimeras.*** RT-PCR was used to quantitate virus as MOI. Stocks of parental virus propagated in MYA-1 cells were similarly titrated for *in vitro* infections. Infections of  $0.5 \times 10^6$  PBMC and MYA-1 with chimeric and parental constructs were performed simultaneously using MOI values of 0.1 and 0.01. Supernatants were collected at 7, 14, or 21 days, and analyzed for production of both viral capsid by ELISA and RNA genomes by real-time PCR.

FIV-PCvif/orfA infections of MYA-1 cells at an MOI of 0.1 resulted in viral RNA levels intermediate to parental constructs by day 7 post-infection (**Fig 3.10a**). At this time FIV-C36 infected cells contained the most viral *gag* equivalents/ml, followed by FIV-PCvif/orfA, then FIV-PPR, and were from highest to lowest:  $3.28 \times 10^7$ ,  $1.46 \times 10^7$ , and  $3.31 \times 10^6$ . Values for all viruses rose over time, and by day 14 post-infection, FIV-PCvif/orfA levels were virtually identical to those of FIV-C36 at  $7.08 \times 10^8$  and  $7.73 \times 10^8$

RNA copies/ ml, while FIV-PPR was  $6.06 \times 10^7$  copies/ ml. Infections using an MOI of 0.01 revealed a similar trend; as expected, by day 7 PI, number of FIV genomes were one order of magnitude lower than infections using MOI of 0.1, with supernatants becoming saturated by day 14 (**Fig 3.10a**).

After one week in PBMC infected at an MOI of 0.1, FIV-PCvif/orfA RNA copies/ ml were lowest, followed by FIV-C36, then FIV-PPR with values of  $6.04 \times 10^4$ ,  $8.44 \times 10^5$ , and  $4.72 \times 10^6$ , respectively (**Fig 3.10b**). FIV-C36 levels rose to  $1.7 \times 10^8$  copies/ ml between one and two weeks, surpassing FIV-PPR which remained relatively constant with a value of  $7.92 \times 10^6$ , as has been observed previously (11-13). Intriguingly, in contrast to results obtained from infection of MYA-1 cells, FIV-PCvif/orfA levels remained lower than either parental virus, only slightly rising to  $1.26 \times 10^5$  copies/ ml by day 14 post-infection, remaining stable through day 21 (**Fig 3.10b**). Further evaluation will be necessary to determine whether this apparent attenuation of FIV-PCvif/orfA in PBMC occurs consistently. As in MYA-1 cell infections, a lower MOI of 0.01 resulted in lower virus production as measured by either ELISA or quantitative RT-PCR.

On day 7 of MYA-1 infections, FIV capsid production was barely above the level of ELISA detection considered positive for all constructs (**Fig 3.11**). By day 14, at MOIs of 0.1 and 0.01, detectable p25 was present, although low during FIV-PPR infections, and nearly equal for FIV-PCvif/orfA and FIV-C36. Infected PBMC supernatant tested via ELISA was negative for both viral doses on days 7, 14, and 21, with only minor signal in some replicates for all constructs (data not shown).

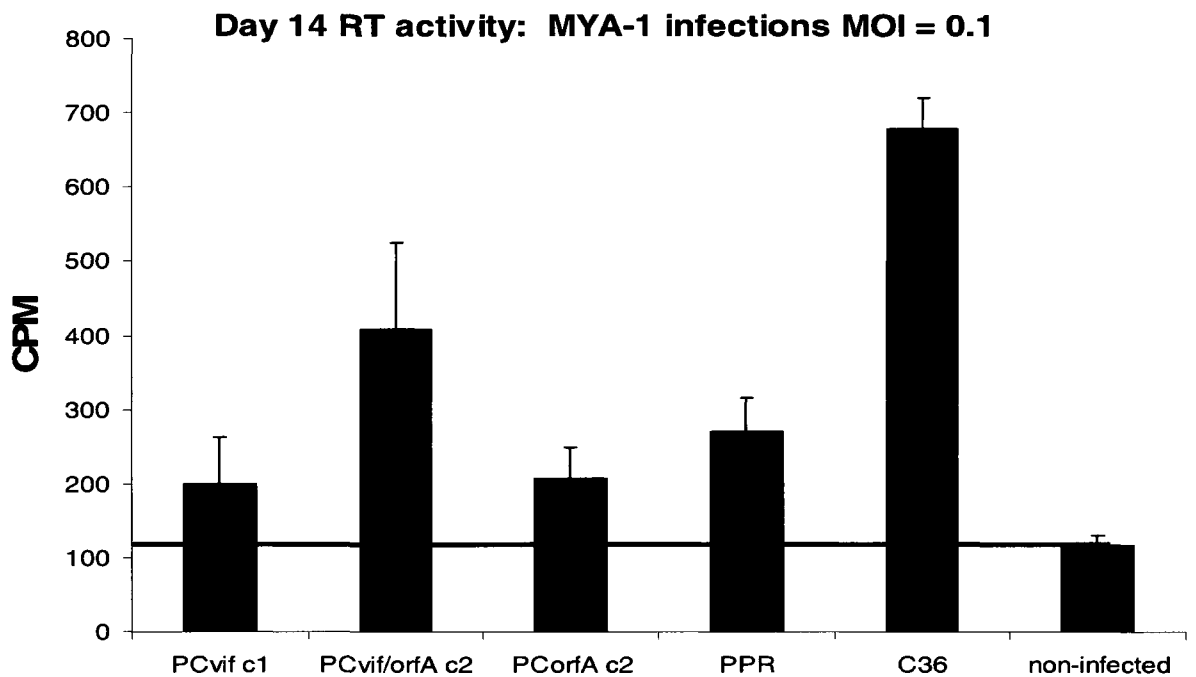


**Figure 3.9:** Relative infections of feline T-cell line MYA-1 by wild-type FIV-PPR and FIV-C36, and chimeric FIV-PCvif, FIV-PCvif/orfA, and FIV-PCorfA. Cells were infected at an MOI of 0.1 as determined by RT-PCR of CrFK transfection supernatants. Reverse transcriptase activity in day 14 post-infection supernatant was recorded as counts per minute using a liquid scintillation counter. Infections were performed in duplicate, RT-assay in triplicate, and means reported here. Red bar denotes background CPM.

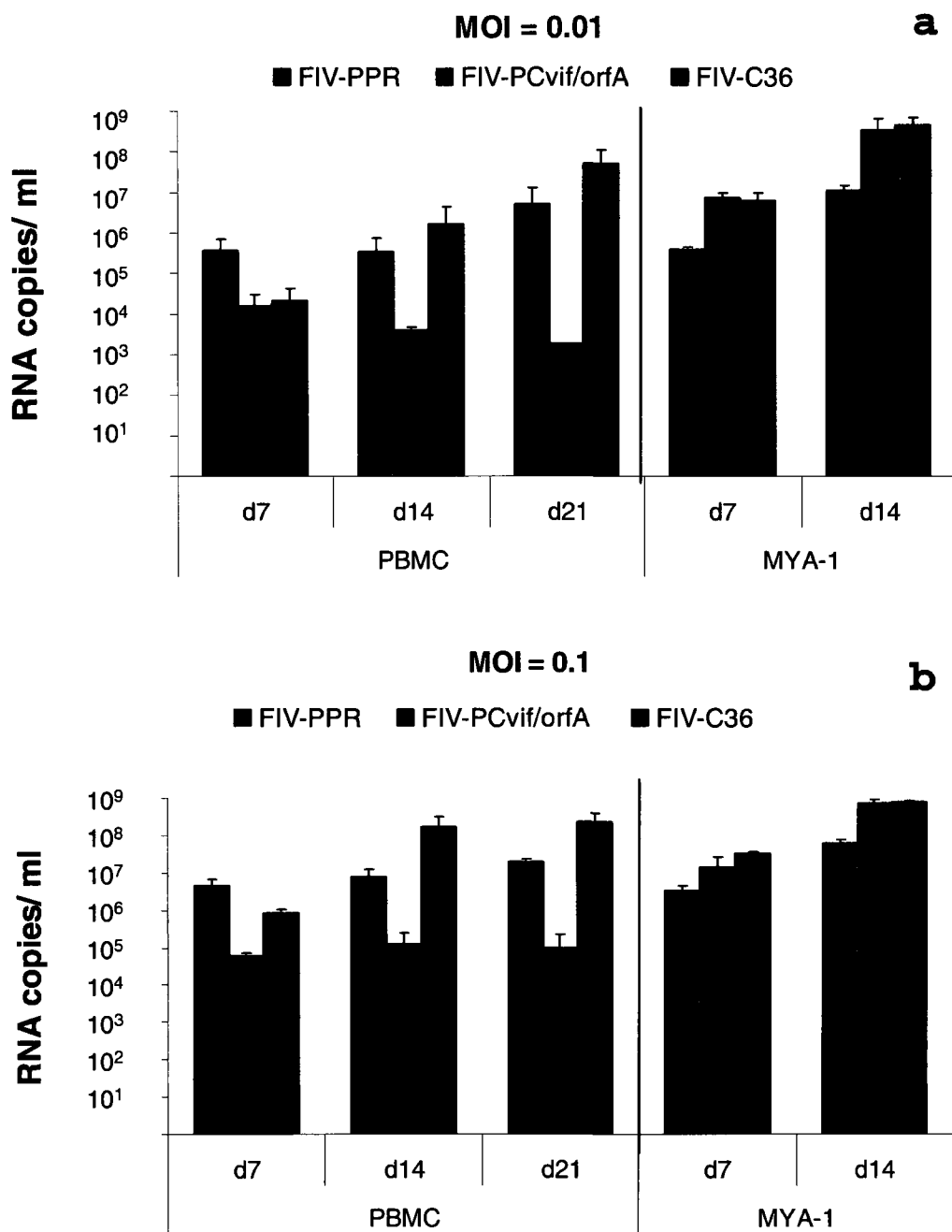


**Figure 3.10:** Relative infections of feline T-cell line MYA-1 and PBMCs by wild-type FIV-PPR and FIV-C36, and chimeric FIV-PCvif/orfA. Cells were infected at MOIs of 0.01 and 0.1 as determined by RT-PCR of MYA-1 generated virus stock. RT-PCR of days 7 and 14 MYA-1 and days 7, 14, and 21 PBMC culture supernatant for detection of FIV genomes. Infections and PCR reactions were performed in triplicate and means reported here.

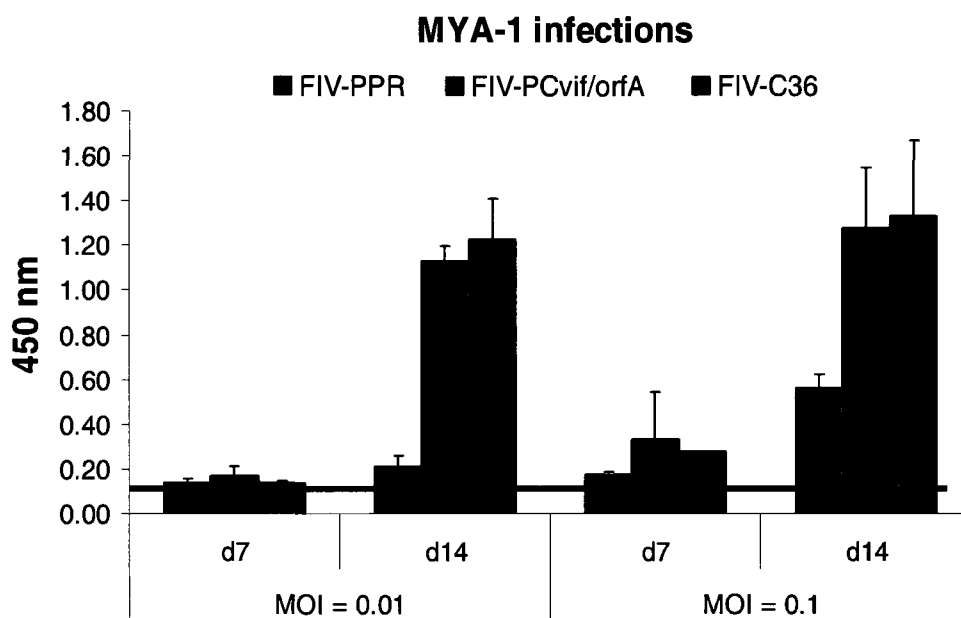


**Figure 3.11:** Relative infections of feline T-cell line MYA-1 by wild-type FIV-PPR and FIV-C36, and chimeric FIV-PCvif/orfA. Cells were infected at MOIs of 0.01 and 0.1 as determined by RT-PCR of virus stock. ELISA assays were performed on days 7 and 14 cell-free culture supernatants to detect FIV p25 antigen. Infections were performed in triplicate, ELISA antigen assay in duplicate, and means reported here. Red bar indicates level of background signal.

## DISCUSSION

We used overlapping-PCR (20) to clone accessory-gene chimeras between the molecular clones FIV-PPR (clade A) and FIV-C36 (clade C). This procedure avoids a major limitation arising from use of restriction enzymes alone to develop viral chimeras. Restriction enzyme-mediated molecular cloning of DNA relies on recognition by the enzyme of specific sites within the DNA, which are typically not present at functional gene junction sites, making generation of single-gene chimeras impossible. We successfully constructed three infectious A/C chimeric FIVs denoted FIV-PCvif, FIV-vif/orfA, and FIV-orfA using the more directed overlapping-PCR technique.

Development of these specific chimeras was undertaken based on *in vivo* replication patterns and associated pathology observed during infections of domestic cats with the clade A/C chimera FIV-PCenv. Based on the intermediate virulence phenotype of FIV-PCenv, we constructed our chimeras to determine whether Vif or OrfA, expressed alone or in tandem, contribute to the highly virulent nature of FIV-C36 (11, 13, 49). Smaller regions of the genome have been substituted to produce FIV-PCvif, FIV-vif/orfA, and FIV-orfA, in hopes that the precise molecular engineering of these constructs may result in increased overall fitness during infections by leaving parental regions that flank functional regulatory genes primarily intact.

Viral infectivity factor, or Vif, is essential for optimal FIV replication both *in vitro* (35, 59, 71) and *in vivo* (24, 62). Similar to its HIV homologue, FIV Vif may have a role in targeting feline APOBEC cytidine deaminases for degradation in the proteasome (7, 37, 61, 79), preventing G-to-A mutations of incoming virus (41, 46, 54, 60). If FIV-C36 Vif functions more efficiently than that of FIV-PPR in disabling feline intracellular

restriction factors, then the chimeras FIV-PCvif or FIV-PCvif/orfA may be able to infect a broader number of target cells, perhaps leading to higher numbers of viral progeny and resultant enhanced virulence *in vivo*. Future experiments to test this hypothesis will include infections in the domestic cat model.

Similar to Vif mutants, FIVs with deletions in *orfA* are attenuated (16, 24, 53, 70). OrfA may have effects on cellular mRNA splicing or proteasome-associated factors (68). Fine-tuning of host cell machinery by OrfA may provide FIV with a mechanism to enhance replication rates through LTR-mediated transcription, or viral assembly, contributing to higher net virion production. The chimeras generated during this study provide an opportunity to explore these possibilities and determine underlying mechanisms of FIV-C36 pathogenicity.

FIV-PPR and FIV-C36 share 83% and 75% nucleotide identity in *vif* and *orfA*, respectively, that translate to 85% and 65% amino acid homology. Thus, it was rational to test whether divergence in coding resulted in phenotypic differences. FIV-PCvif, FIV-PCvif/orfA, and FIV-PCorfA were all infectious *in vitro* as determined by RT-activity in the supernatant of infected MYA-1 cells. A more comprehensive set of FIV-PCvif/orfA infections revealed that replicative ability as measured by RNA genome and capsid production was nearly equal to that of FIV-C36 when performed in the CD4<sup>+</sup>CD25<sup>+</sup> T-cell line, MYA-1. However, preliminary experiments indicate this phenomenon may be cell-type dependent, as primary feline PBMC were refractory to infection with FIV-PCvif/orfA relative to parental strains.

Future work will include generation of high-titer stocks of FIV-PCorfA and FIV-PCvif, along with more extensive testing of all three chimeras in stimulated and

unstimulated bulk PBMC, and individual PBMC cell types (ie. CD4<sup>+</sup>, CD8<sup>+</sup> T-cells and macrophages) from feline peripheral blood. It will also be valuable to test infectivity of FIV-PCorfA, FIV-PCvif/orfA, and FIV-PCvif in additional cell types to relate accessory-gene function to the ability of viruses to replicate in different cell environments.

Additional *in vitro* studies include evaluation of: cytokine induction, cellular activation and changes in cell-surface phenotype, viral mRNA processing and transport, virion assembly and budding, and G→A mutations arising after reverse-transcription.

If further *in vitro* studies confirm preliminary observations that all three chimeras are replication-competent, it will be highly informative to perform *in vivo* studies to determine activity of accessory-gene substitutions in a whole animal model. Thus, the constructs generated and tested in preliminary trials as described here offer great potential for discovery of important aspects of lentiviral pathogenesis.

## CONCLUSION

FIV infection of the domestic cat offers a model system for basic biological research of lentivirus-induced immunodeficiencies, along with development of treatments for HIV-AIDS. Two strains of FIV, FIV-PPR and FIV-C36 have been molecularly cloned and studied in relationship to severity of disease following productive infection. Higher viral titers and more rapid onset of clinical symptoms are observed during experimental infections with FIV-C36 compared to FIV-PPR. FIV-C36, a highly pathogenic molecular clone of the clade C FIV isolate FIV-PGammar, differs in genetic sequence from the clade A molecular clone FIV-PPR by about 15%. Therefore, it is rational to believe that infections of the domestic cat with molecular chimeras between FIV strains possessing differing pathogenic phenotypes can help identify which genetic elements contribute to progression to AIDS.

Mutations of the FIV envelope gene occur more frequently than changes in other regions of the genome. Structural components of a lentivirus encoded by *gag*, and enzymes found on *pol* such as reverse transcriptase, have evolved over time to function in concert with cellular elements in a way that has proved efficacious for virus propagation. As a result, mutations to these regions generally prove more detrimental to overall viral fitness, and therefore quasispecies with changes in *gag* or *pol* elements are less likely to replicate effectively. Hypervariable regions within *env* however, are more resilient. Further, mutations that do not affect critical binding and fusion events can result in outgrowth of a number of quasispecies that may elude immune surveillance.

A series of chimeras between FIV-C36 and FIV-PPR was developed to evaluate phenotype, and to assess whether genomic elements from FIV-C36 conferred enhanced virulence to these mutant constructs. FIV-PCenv, a chimera in which much of the 3' half of the FIV-C36 genome, including *env*, was swapped with that of FIV-PPR, was chosen for further *in vivo* characterization. Since relative CD134 and CXCR4 binding affinities of Env from FIV-PPR and FIV-C36 were shown to be identical by a series of *in vitro* assays, properties other than receptor binding affinity required further investigation as the mechanism for enhanced *in vivo* pathogenicity of FIV-C36. Induction of host immune response to Env, or expression of the FIV-C36 regulatory elements Vif and OrfA by the chimera, were considered logical future directions. Results from the *in vivo* study detailed in Chapter One show an initial delay in replication potential of FIV-PCenv, after which proviral loads in peripheral blood and bone marrow were equal to those of FIV-PPR. Because viral genetic manipulation of chimeras can result in attenuation (as observed with the other chimera tested, FIV-PC3'LTR), demonstration that FIV-PCenv had enhanced virulence relative to FIV-PPR led to consideration of additional investigations. FIV-PCenv infections resulted in plasma viremia levels and hematologic effects intermediate to parental strains, supporting the hypothesis that FIV-C36 genomic elements are molecular determinants of virulence.

Upon passage of FIV-PCenv into a second cohort of animals, described in Chapter Two, replication kinetics were not delayed, suggesting adaptation of the chimera during primary infection, leading to stabilization of *in vivo* growth capacity. Further evidence for adaptation is provided by viral load data. While initial spikes of FIV-PCenv-induced viremia were not as high as FIV-C36, higher levels of both provirus and

circulating virus were detected early in FIV-PCenv infected cats compared to FIV-PPR. During the primary study, the chimera showed an intermediate phenotype; however, *in vivo* passage resulted in prolonged maintenance of integrated and circulating virus in peripheral blood.

Lentiviruses, including FIV, have evolved regulatory proteins which play important roles in viral replication and likely in pathogenesis. These factors are encoded in the 3' half of the genome. They serve functions which assist various stages of viral propagation, allowing for increased efficiency, and production of larger numbers of progeny from an individual infected cell. Further, some of these accessory proteins, such as Vif, play a role in the regulation of innate, intracellular antiviral responses.

Given the results from experiments with FIV-PCenv, it was hypothesized that FIV regulatory elements could be responsible for the highly virulent phenotype of FIV-C36. As described in Chapter Three, a panel of FIV regulatory-gene chimeras, containing FIV-C36 *vif*, *orfA*, or *vif* and *orfA* in tandem on the FIV-PPR backbone were developed. FIV-PCvif, FIV-PCorfA, and FIV-PC-vif/orfA chimeras were cloned using PCR-driven overlap extension to target specific replacement of FIV-PPR accessory genes. Sequencing confirmed the appropriate identity of all constructs, and plasmids were transfected into feline cells to generate infectious viral particles. Supernatants harvested from transfection experiments were all infectious in the feline lymphoid cell line MYA-1. Subsequent titered infections with FIV-PCvif/orfA resulted in levels of virion production higher than FIV-PPR and equal to FIV-C36 in MYA-1 cells, suggesting the importance of these regulatory elements for enhanced viral replication capacity. These findings may result from an increase in the number of viral progeny mediated by OrfA effects on

transcription rates from viral LTR. Vif function may contribute to the ability of FIV-PCvif/orfA to productively infect more cells by avoiding extensive G→A mutations, and other detrimental effects imposed by APOBEC-like factors or other innate intracellular restriction mechanisms. In contrast, infection of PBMC resulted in less replication than both parental viruses, possibly due to anti-viral factors inherent to a particular cell type found within the milieu present in whole blood.

Future testing of the ability of accessory-gene chimeras to infect whole feline PBMC, along with sorted peripheral cell types will provide insight into the effects of these gene products on FIV infectivity of primary cells. Additionally, induction of cytokines and other immune modulators produced by infected cells can be measured to assess non-cellular modulators of host immunity. Based on preliminary *ex vivo* data, *in vivo* challenge experiments could be initiated to assess the ability of Vif and OrfA chimeras to induce disease, and further define the impact of these factors during development of immunodeficiency.

## REFERENCES

1. **Balfe, P., S. Shapiro, M. Hsu, C. Buckner, J. M. Harouse, and C. Cheng-Mayer.** 2004. Expansion of quasispecies diversity but no evidence for adaptive evolution of SHIV during rapid serial transfers among seronegative macaques. *Virology* **318**:267-79.
2. **Bishop, S. A., C. R. Stokes, T. J. Gruffydd-Jones, C. V. Whiting, and D. A. Harbour.** 1996. Vaginal and rectal infection of cats with feline immunodeficiency virus. *Vet Microbiol* **51**:217-27.
3. **Burkhard, M. J., and G. A. Dean.** 2003. Transmission and immunopathogenesis of FIV in cats as a model for HIV. *Curr HIV Res* **1**:15-29.
4. **Burkhard, M. J., C. K. Mathiason, T. Bowdre, and E. A. Hoover.** 2001. Feline immunodeficiency virus Gag- and Env-specific immune responses after vaginal versus intravenous infection. *AIDS Res Hum Retroviruses* **17**:1767-78.
5. **Chatterji, U., A. de Parseval, and J. H. Elder.** 2002. Feline immunodeficiency virus OrfA is distinct from other lentivirus transactivators. *J Virol* **76**:9624-34.
6. **Coffin, J., S. Hughes, and H. Varmus (ed.).** 1997. *Retroviruses*, First ed. Cold Spring Harbor Laboratory Press.
7. **Conticello, S. G., R. S. Harris, and M. S. Neuberger.** 2003. The Vif protein of HIV triggers degradation of the human antiretroviral DNA deaminase APOBEC3G. *Curr Biol* **13**:2009-13.
8. **Crandell, R. A., C. G. Fabricant, and W. A. Nelson-Rees.** 1973. Development, characterization, and viral susceptibility of a feline (*Felis catus*) renal cell line (CRFK). *In Vitro* **9**:176-85.
9. **de Parseval, A., U. Chatterji, P. Sun, and J. H. Elder.** 2004. Feline immunodeficiency virus targets activated CD4+ T cells by using CD134 as a binding receptor. *Proc Natl Acad Sci U S A* **101**:13044-9.
10. **de Parseval, A., and J. H. Elder.** 1999. Demonstration that orf2 encodes the feline immunodeficiency virus transactivating (Tat) protein and characterization of a unique gene product with partial rev activity. *J Virol* **73**:608-17.
11. **de Rozieres, S., C. K. Mathiason, M. R. Rolston, U. Chatterji, E. A. Hoover, and J. H. Elder.** 2004. Characterization of a highly pathogenic molecular clone of feline immunodeficiency virus clade C. *J Virol* **78**:8971-82.

12. **de Rozieres, S., J. Thompson, M. Sundstrom, J. Gruber, D. S. Stump, A. P. de Parseval, S. VandeWoude, and J. H. Elder.** 2008. Replication properties of clade A/C chimeric feline immunodeficiency viruses and evaluation of infection kinetics in the domestic cat. *J Virol* **82**:7953-63.
13. **Diehl, L. J., C. K. Mathiason-Dubard, L. L. O'Neil, L. A. Obert, and E. A. Hoover.** 1995. Induction of accelerated feline immunodeficiency virus disease by acute-phase virus passage. *J Virol* **69**:6149-57.
14. **Duarte, A., and L. Tavares.** 2006. Phylogenetic analysis of Portuguese Feline Immunodeficiency Virus sequences reveals high genetic diversity. *Vet Microbiol* **114**:25-33.
15. **English, R. V., P. Nelson, C. M. Johnson, M. Nasisse, W. A. Tompkins, and M. B. Tompkins.** 1994. Development of clinical disease in cats experimentally infected with feline immunodeficiency virus. *J Infect Dis* **170**:543-52.
16. **Gemeniano, M. C., E. T. Sawai, C. M. Leutenegger, and E. E. Sparger.** 2003. Feline immunodeficiency virus ORF-Ais required for virus particle formation and virus infectivity. *J Virol* **77**:8819-30.
17. **Gemeniano, M. C., E. T. Sawai, and E. E. Sparger.** 2004. Feline immunodeficiency virus Orf-A localizes to the nucleus and induces cell cycle arrest. *Virology* **325**:167-74.
18. **Goldstein, S., R. Engle, R. A. Olmsted, V. M. Hirsch, and P. R. Johnson.** 1990. Detection of SIV antigens by HIV-1 antigen capture immunoassays. *J Acquir Immune Defic Syndr* **3**:98-102.
19. **Hatzioannou, T., D. Perez-Caballero, A. Yang, S. Cowan, and P. D. Bieniasz.** 2004. Retrovirus resistance factors Ref1 and Lv1 are species-specific variants of TRIM5alpha. *Proc Natl Acad Sci U S A* **101**:10774-9.
20. **Heckman, K. L., and L. R. Pease.** 2007. Gene splicing and mutagenesis by PCR-driven overlap extension. *Nat Protoc* **2**:924-32.
21. **Hokanson, R. M., J. TerWee, I. S. Choi, J. Coates, H. Dean, D. N. Reddy, A. M. Wolf, and E. W. Collisson.** 2000. Dose response studies of acute feline immunodeficiency virus PPR strain infection in cats. *Vet Microbiol* **76**:311-27.
22. **Ikeda, Y., K. Tomonaga, Y. Kawaguchi, M. Kohmoto, Y. Inoshima, Y. Tohya, T. Miyazawa, C. Kai, and T. Mikami.** 1996. Feline immunodeficiency virus can infect a human cell line (MOLT-4) but establishes a state of latency in the cells. *J Gen Virol* **77 ( Pt 8)**:1623-30.

23. **Inoshima, Y., M. Kohmoto, Y. Ikeda, H. Yamada, Y. Kawaguchi, K. Tomonaga, T. Miyazawa, C. Kai, T. Umemura, and T. Mikami.** 1996. Roles of the auxiliary genes and AP-1 binding site in the long terminal repeat of feline immunodeficiency virus in the early stage of infection in cats. *J Virol* **70**:8518-26.
24. **Inoshima, Y., T. Miyazawa, and T. Mikami.** 1998. The roles of vif and ORF-A genes and AP-1 binding site in in vivo replication of feline immunodeficiency virus. *Arch Virol* **143**:789-95.
25. **Ishida, T., T. Washizu, K. Toriyabe, S. Motoyoshi, I. Tomoda, and N. C. Pedersen.** 1989. Feline immunodeficiency virus infection in cats of Japan. *J Am Vet Med Assoc* **194**:221-5.
26. **Johnston, J. B., C. Silva, and C. Power.** 2002. Envelope gene-mediated neurovirulence in feline immunodeficiency virus infection: induction of matrix metalloproteinases and neuronal injury. *J Virol* **76**:2622-33.
27. **Kakinuma, S., K. Motokawa, T. Hohdatsu, J. K. Yamamoto, H. Koyama, and H. Hashimoto.** 1995. Nucleotide sequence of feline immunodeficiency virus: classification of Japanese isolates into two subtypes which are distinct from non-Japanese subtypes. *J Virol* **69**:3639-46.
28. **Kann, R., J. Seddon, M. Kyaw-Tanner, J. P. Schoeman, T. Schoeman, and J. Meers.** 2006. Phylogenetic analysis to define feline immunodeficiency virus subtypes in 31 domestic cats in South Africa. *J S Afr Vet Assoc* **77**:108-13.
29. **Kann, R. K., M. T. Kyaw-Tanner, J. M. Seddon, P. R. Lehrbach, R. J. Zwijnenberg, and J. Meers.** 2006. Molecular subtyping of feline immunodeficiency virus from domestic cats in Australia. *Aust Vet J* **84**:112-6.
30. **Kohmoto, M., T. Miyazawa, K. Tomonaga, Y. Kawaguchi, T. Mori, Y. Tohya, C. Kai, and T. Mikami.** 1994. Comparison of biological properties of feline immunodeficiency virus isolates using recombinant chimeric viruses. *J Gen Virol* **75 ( Pt 8)**:1935-42.
31. **Kozyrev, I. L., K. Ibuki, T. Shimada, T. Kuwata, T. Takemura, M. Hayami, and T. Miura.** 2001. Characterization of less pathogenic infectious molecular clones derived from acute-pathogenic SHIV-89.6p stock virus. *Virology* **282**:6-13.
32. **Kusuhara, H., T. Hohdatsu, M. Okumura, K. Sato, Y. Suzuki, K. Motokawa, T. Gemma, R. Watanabe, C. Huang, S. Arai, and H. Koyama.** 2005. Dual-subtype vaccine (Fel-O-Vax FIV) protects cats against contact challenge with heterologous subtype B FIV infected cats. *Vet Microbiol* **108**:155-65.

33. **Li, J. T., M. Halloran, C. I. Lord, A. Watson, J. Ranchalis, M. Fung, N. L. Letvin, and J. G. Sodroski.** 1995. Persistent infection of macaques with simian-human immunodeficiency viruses. *J Virol* **69**:7061-7.
34. **Lochelt, M., F. Romen, P. Bastone, H. Muckenfuss, N. Kirchner, Y. B. Kim, U. Truyen, U. Rosler, M. Battenberg, A. Saib, E. Flory, K. Cichutek, and C. Munk.** 2005. The antiretroviral activity of APOBEC3 is inhibited by the foamy virus accessory Bet protein. *Proc Natl Acad Sci U S A* **102**:7982-7.
35. **Lockridge, K. M., S. Himathongkham, E. T. Sawai, M. Chienand, and E. E. Sparger.** 1999. The feline immunodeficiency virus vif gene is required for productive infection of feline peripheral blood mononuclear cells and monocyte-derived macrophages. *Virology* **261**:25-30.
36. **Luciw, P. A., E. Pratt-Lowe, K. E. Shaw, J. A. Levy, and C. Cheng-Mayer.** 1995. Persistent infection of rhesus macaques with T-cell-line-tropic and macrophage-tropic clones of simian/human immunodeficiency viruses (SHIV). *Proc Natl Acad Sci U S A* **92**:7490-4.
37. **Marin, M., K. M. Rose, S. L. Kozak, and D. Kabat.** 2003. HIV-1 Vif protein binds the editing enzyme APOBEC3G and induces its degradation. *Nat Med* **9**:1398-403.
38. **Mergia, A., J. Blackwell, and S. Chari.** 1997. Inhibition of FIV replication by a ribozyme that targets the Rev response element. *AIDS Res Hum Retroviruses* **13**:1333-9.
39. **Miyazawa, T., T. Furuya, S. Itagaki, Y. Tohya, E. Takahashi, and T. Mikami.** 1989. Establishment of a feline T-lymphoblastoid cell line highly sensitive for replication of feline immunodeficiency virus. *Arch Virol* **108**:131-5.
40. **Moench, T. R., K. J. Whaley, T. D. Mandrell, B. D. Bishop, C. J. Witt, and R. A. Cone.** 1993. The cat/feline immunodeficiency virus model for transmucosal transmission of AIDS: nonoxynol-9 contraceptive jelly blocks transmission by an infected cell inoculum. *AIDS* **7**:797-802.
41. **Munk, C., J. Zielonka, H. Constabel, B. P. Kloke, B. Rengstl, M. Battenberg, F. Bonci, M. Pistello, M. Lochelt, and K. Cichutek.** 2007. Multiple restrictions of human immunodeficiency virus type 1 in feline cells. *J Virol* **81**:7048-60.
42. **Nakamura, K., Y. Suzuki, K. Ikeo, Y. Ikeda, E. Sato, N. T. Nguyen, T. Gojobori, T. Mikami, and T. Miyazawa.** 2003. Phylogenetic analysis of Vietnamese isolates of feline immunodeficiency virus: genetic diversity of subtype C. *Arch Virol* **148**:783-91.

43. **Novak, J. M., P. C. Crawford, H. M. Kolenda-Roberts, C. M. Johnson, and A. Mergia.** 2007. Viral gene expression and provirus load of Orf-A defective FIV in lymphoid tissues and lymphocyte subpopulations of neonatal cats during acute and chronic infections. *Virus Res* **130**:110-20.
44. **Nowak, M. A., R. M. May, and R. M. Anderson.** 1990. The evolutionary dynamics of HIV-1 quasispecies and the development of immunodeficiency disease. *AIDS* **4**:1095-103.
45. **Obert, L. A., and E. A. Hoover.** 2000. Feline immunodeficiency virus clade C mucosal transmission and disease courses. *AIDS Res Hum Retroviruses* **16**:677-88.
46. **Paul, T. A., J. W. Casey, R. J. Avery, and C. A. Sutton.** 2007. Expression of feline immunodeficiency virus Vif is associated with reduced viral mutation rates without restoration of replication of vif mutant viruses. *Virology* **361**:112-22.
47. **Pecoraro, M. R., K. Tomonaga, T. Miyazawa, Y. Kawaguchi, S. Sugita, Y. Tohya, C. Kai, M. E. Etcheverrigaray, and T. Mikami.** 1996. Genetic diversity of Argentine isolates of feline immunodeficiency virus. *J Gen Virol* **77 ( Pt 9)**:2031-5.
48. **Pedersen, N. C., E. W. Ho, M. L. Brown, and J. K. Yamamoto.** 1987. Isolation of a T-lymphotropic virus from domestic cats with an immunodeficiency-like syndrome. *Science* **235**:790-3.
49. **Pedersen, N. C., C. M. Leutenegger, J. Woo, and J. Higgins.** 2001. Virulence differences between two field isolates of feline immunodeficiency virus (FIV-APetaluma and FIV-CPGammar) in young adult specific pathogen free cats. *Vet Immunol Immunopathol* **79**:53-67.
50. **Pedersen, N. C., J. K. Yamamoto, T. Ishida, and H. Hansen.** 1989. Feline immunodeficiency virus infection. *Vet Immunol Immunopathol* **21**:111-29.
51. **Phillips, T. R., C. Lamont, D. A. Konings, B. L. Shacklett, C. A. Hamson, P. A. Luciw, and J. H. Elder.** 1992. Identification of the Rev transactivation and Rev-responsive elements of feline immunodeficiency virus. *J Virol* **66**:5464-71.
52. **Phillips, T. R., R. L. Talbott, C. Lamont, S. Muir, K. Lovelace, and J. H. Elder.** 1990. Comparison of two host cell range variants of feline immunodeficiency virus. *J Virol* **64**:4605-13.
53. **Pistello, M., M. Moscardini, P. Mazzetti, F. Bonci, L. Zaccaro, P. Isola, G. Freer, S. Specter, D. Matteucci, and M. Bendinelli.** 2002. Development of feline immunodeficiency virus ORF-A (tat) mutants: in vitro and in vivo characterization. *Virology* **298**:84-95.

54. **Poss, M., H. A. Ross, S. L. Painter, D. C. Holley, J. A. Terwee, S. Vandewoude, and A. Rodrigo.** 2006. Feline lentivirus evolution in cross-species infection reveals extensive G-to-A mutation and selection on key residues in the viral polymerase. *J Virol* **80**:2728-37.
55. **Pu, R., J. Coleman, M. Omori, M. Arai, T. Hohdatsu, C. Huang, T. Tanabe, and J. K. Yamamoto.** 2001. Dual-subtype FIV vaccine protects cats against in vivo swarms of both homologous and heterologous subtype FIV isolates. *AIDS* **15**:1225-37.
56. **Reimann, K. A., J. T. Li, R. Veazey, M. Halloran, I. W. Park, G. B. Karlsson, J. Sodroski, and N. L. Letvin.** 1996. A chimeric simian/human immunodeficiency virus expressing a primary patient human immunodeficiency virus type 1 isolate env causes an AIDS-like disease after in vivo passage in rhesus monkeys. *J Virol* **70**:6922-8.
57. **Richardson, J., G. Pancino, R. Merat, T. Leste-Lasserre, A. Moraillon, J. Schneider-Mergener, M. Alizon, P. Sonigo, and N. Heveker.** 1999. Shared usage of the chemokine receptor CXCR4 by primary and laboratory-adapted strains of feline immunodeficiency virus. *J Virol* **73**:3661-71.
58. **Saenz, D. T., W. Teo, J. C. Olsen, and E. M. Poeschla.** 2005. Restriction of feline immunodeficiency virus by Ref1, Lv1, and primate TRIM5alpha proteins. *J Virol* **79**:15175-88.
59. **Shacklett, B. L., and P. A. Luciw.** 1994. Analysis of the vif gene of feline immunodeficiency virus. *Virology* **204**:860-7.
60. **Sheehy, A. M., N. C. Gaddis, J. D. Choi, and M. H. Malim.** 2002. Isolation of a human gene that inhibits HIV-1 infection and is suppressed by the viral Vif protein. *Nature* **418**:646-50.
61. **Sheehy, A. M., N. C. Gaddis, and M. H. Malim.** 2003. The antiretroviral enzyme APOBEC3G is degraded by the proteasome in response to HIV-1 Vif. *Nat Med* **9**:1404-7.
62. **Shen, X., C. M. Leutenegger, K. Stefano Cole, N. C. Pedersen, and E. E. Sparger.** 2007. A feline immunodeficiency virus vif-deletion mutant remains attenuated upon infection of newborn kittens. *J Gen Virol* **88**:2793-9.
63. **Shimajima, M., T. Miyazawa, Y. Ikeda, E. L. McMonagle, H. Haining, H. Akashi, Y. Takeuchi, M. J. Hosie, and B. J. Willett.** 2004. Use of CD134 as a primary receptor by the feline immunodeficiency virus. *Science* **303**:1192-5.
64. **Slaughter, M. R., J. M. Birmingham, B. Patel, G. A. Whelan, A. J. Krebs-Brown, P. D. Hockings, and J. A. Osborne.** 2002. Extended acclimatization is

required to eliminate stress effects of periodic blood-sampling procedures on vasoactive hormones and blood volume in beagle dogs. *Lab Anim* **36**:403-10.

65. **Sodora, D. L., E. G. Shpaer, B. E. Kitchell, S. W. Dow, E. A. Hoover, and J. I. Mullins.** 1994. Identification of three feline immunodeficiency virus (FIV) env gene subtypes and comparison of the FIV and human immunodeficiency virus type 1 evolutionary patterns. *J Virol* **68**:2230-8.
66. **Sparger, E. E., A. M. Beebe, N. Dua, S. Himathongkam, J. H. Elder, M. Torten, and J. Higgins.** 1994. Infection of cats with molecularly cloned and biological isolates of the feline immunodeficiency virus. *Virology* **205**:546-53.
67. **Stremlau, M., C. M. Owens, M. J. Perron, M. Kiessling, P. Autissier, and J. Sodroski.** 2004. The cytoplasmic body component TRIM5alpha restricts HIV-1 infection in Old World monkeys. *Nature* **427**:848-53.
68. **Sundstrom, M., U. Chatterji, L. Schaffer, S. de Rozieres, and J. H. Elder.** 2008. Feline immunodeficiency virus OrfA alters gene expression of splicing factors and proteasome-ubiquitination proteins. *Virology* **371**:394-404.
69. **Tomonaga, K., and T. Mikami.** 1996. Molecular biology of the feline immunodeficiency virus auxiliary genes. *J Gen Virol* **77 ( Pt 8)**:1611-21.
70. **Tomonaga, K., T. Miyazawa, J. Sakuragi, T. Mori, A. Adachi, and T. Mikami.** 1993. The feline immunodeficiency virus ORF-A gene facilitates efficient viral replication in established T-cell lines and peripheral blood lymphocytes. *J Virol* **67**:5889-95.
71. **Tomonaga, K., J. Norimine, Y. S. Shin, M. Fukasawa, T. Miyazawa, A. Adachi, T. Toyosaki, Y. Kawaguchi, C. Kai, and T. Mikami.** 1992. Identification of a feline immunodeficiency virus gene which is essential for cell-free virus infectivity. *J Virol* **66**:6181-5.
72. **Tomonaga, K., Y. S. Shin, M. Fukasawa, T. Miyazawa, A. Adachi, and T. Mikami.** 1993. Feline immunodeficiency virus gene expression: analysis of the RNA splicing pattern and the monocistronic rev mRNA. *J Gen Virol* **74 ( Pt 11)**:2409-17.
73. **Troyer, J. L., J. Pecon-Slattery, M. E. Roelke, W. Johnson, S. VandeWoude, N. Vazquez-Salat, M. Brown, L. Frank, R. Woodroffe, C. Winterbach, H. Winterbach, G. Hemson, M. Bush, K. A. Alexander, E. Revilla, and S. J. O'Brien.** 2005. Seroprevalence and genomic divergence of circulating strains of feline immunodeficiency virus among Felidae and Hyaenidae species. *J Virol* **79**:8282-94.

74. **Waters, A. K., A. P. De Parseval, D. L. Lerner, J. C. Neil, F. J. Thompson, and J. H. Elder.** 1996. Influence of ORF2 on host cell tropism of feline immunodeficiency virus. *Virology* **215**:10-6.
75. **Willett, B. J., L. Picard, M. J. Hosie, J. D. Turner, K. Adema, and P. R. Clapham.** 1997. Shared usage of the chemokine receptor CXCR4 by the feline and human immunodeficiency viruses. *J Virol* **71**:6407-15.
76. **Willey, R. L., D. H. Smith, L. A. Lasky, T. S. Theodore, P. L. Earl, B. Moss, D. J. Capon, and M. A. Martin.** 1988. In vitro mutagenesis identifies a region within the envelope gene of the human immunodeficiency virus that is critical for infectivity. *J Virol* **62**:139-47.
77. **Yamamoto, J. K., H. Hansen, E. W. Ho, T. Y. Morishita, T. Okuda, T. R. Sawa, R. M. Nakamura, and N. C. Pedersen.** 1989. Epidemiologic and clinical aspects of feline immunodeficiency virus infection in cats from the continental United States and Canada and possible mode of transmission. *J Am Vet Med Assoc* **194**:213-20.
78. **Yamamoto, J. K., E. Sparger, E. W. Ho, P. R. Andersen, T. P. O'Connor, C. P. Mandell, L. Lowenstine, R. Munn, and N. C. Pedersen.** 1988. Pathogenesis of experimentally induced feline immunodeficiency virus infection in cats. *Am J Vet Res* **49**:1246-58.
79. **Yu, X., Y. Yu, B. Liu, K. Luo, W. Kong, P. Mao, and X. F. Yu.** 2003. Induction of APOBEC3G ubiquitination and degradation by an HIV-1 Vif-Cul5-SCF complex. *Science* **302**:1056-60.